Studies on the *Om(1E)* locus of *Drosophila ananassae*

Naoto Juni

Studies on the *Om(1E)* locus of *Drosophila ananassae*

Naoto Juni

A thesis presented to the Graduate School of Science of Hokkaido University, in partial fulfillment of the requirements for the degree of Doctor of Science.

1995, Sapporo

CONTENTS

ACKNOWLEDGMENTS 1

ABSTRACT 2

INTRODUCTION 3

Chapter I. Description of the *Om(1E)* phenotype 7

INTRODUCTION 8

MATERIALS AND METHODS 8

RESULTS 10

DISCUSSION 17

Chapter II. Molecular genetics of the *Om(1E)* locus 18

INTRODUCTION 19

MATERIALS AND METHODS 19

RESULTS 23

DISCUSSION 41

Chapter III. Spatial expression of the *Om(1E)* gene 42

INTRODUCTION 43

MATERIALS AND METHODS 43

RESULTS 48

DISCUSSION 60

GENERAL DISCUSSION 62

REFERENCES 70

ACKNOWLEDGMENTS

Grateful acknowledgment is made to Professor Samuel H. Hori, Hokkaido University, for his instruction and encouragement in the course of this study; to Kiyohito Yoshida and Takeshi Awasaki for stimulative discussion and experimental assistance through the course of this study; to Claude W. Hinton, Yoshiko N. Tobari, and Hiroshi Matsubayashi for providing *Drosophila ananassae* stocks and genetical information; to Victor G. Corces for the *ras2* gene probe and plasmids for *P*-element-mediated transformation; to Shinobu C. Fujita for MAb22C10; to Ken-ichi Kimura, Kazuya Usui, Hiroki Ito, Naoto Kagiyama, and Takashi Hamabata for technical advice; to Masahito T. Kimura and Takao Yoshida for their help in preparation of the thesis.

ABSTRACT

Optic morphology (*Om*) mutations in *Drosophila ananassae* are a group of retrotransposon (*tom*)-induced gain-of-function mutations which map to at least 22 independent loci and exclusively affect the compound eye morphology. Unlike all the other *Om* mutants which are characterized by fewer-than-normal and disorganized ommatidia, the *Om(1E)* mutants exceptionally possess enlarged compound eyes, giving impression that one extra eye is fused dorso-posteriorly to another.

In order to characterize the *Om(1E)* mutation and the *Om(1E)* gene, I have carried out molecular analyses. A putative *Om(1E)* locus cloned by *tom*-tagging and chromosome walking contained two transcribed regions in the vicinity of *tom* insertion sites of the *Om(1E)* mutant alleles, and one of these regions was shown to be the *Om(1E)* gene by analyses of gene expression patterns in wild-type and the mutants, and by production of the phenocopy by *P*-element-mediated transformation with *Drosophila melanogaster*. Sequence analysis showed that the *Om(1E)* gene encodes a novel protein having potential transmembrane domain(s). *in situ* hybridization and immunocytochemical analyses demonstrated that the *Om(1E)* gene is expressed ubiquitously in embryonic cells, imaginal discs, and the central nervous system of third instar larvae, and specifically in lamina precursor cells. Artificial ubiquitous over-expression of *Om(1E)* or its antisense RNA affected morphogenesis of wing imaginal disc derivatives and/or large bristle formation. These findings suggest that the *Om(1E)* gene is involved in various biological events.

INTRODUCTION

Many of spontaneous mutations are caused by the insertion of transposons (for reviews, see Shapiro, 1983; Georgiev, 1984). In the majority of cases, transposon-insertional mutations result in complete or partial loss-of-function by disrupting gene structure or by suppressing gene expression. However, there exist several cases in which transposon insertions cause dominant gain-of-function mutations by activating expression of adjacent genes. For example, gene expression is activated by the Ty1 element in the yeast ROAM (regulated overproducing alleles under mating signals) mutations (for a review, see Boeke, 1989), by the Mu and the Ds elements in the *Knotted* (*Kn1*) mutation of maize (Hake, 1992), by the Tam3 element in the ovulata mutation of Antirrhinum (Bradley et al., 1993), by the *gypsy* and the *copia* retrotransposons in the *Hairy-wing* (*Hw*) mutation of *Drosophila melanogaster* (Campuzano et al., 1986), and by defective *P* elements in the glucose-6-phosphate dehydrogenase (G6PD) high activity mutation of *Drosophila melanogaster* (Itoh et al., 1988; Ito et al., 1989). It is also included in this category that tumorigenesis in vertebrates is sometimes induced by proviral insertions of retroviruses which activate expression of proto-oncogenes in the ways called "promoter insertion mode" or "enhancer insertion mode" (for a review, see Nusse, 1986). Such mutations often enable us to recognize hidden genes and their functions.

Optic morphology (*Om*) mutations in *Drosophila ananassae* are another example of gain-of-function mutations resulting from enhanced expression of relevant genes by transposon insertion; *Om* mutations are a group of semidominant mutations mapped to at least 22 independent loci which exclusively display abnormalities of the compound eye morphology

(Hinton, 1984). *Om* mutants were first recovered from the progeny of females of a particular marker stock, *claret; plexus* (*ca; px*) at a frequency of $2x10^{-4}$. Most of the loci were represented by more than two *Om* mutants which sometimes display locus-specific phenotype, though inter-locus mimicry was not rare. Based on these and other observations, Hinton (1984) speculated that a hypothetical transposable element (*tom*) might be responsible for *Om* mutations which specifically inserts into control sequences shared by a set of structural genes involved in eye morphogenesis. Subsequent studies on these mutations have revealed that the *tom* element is indeed present as a 7-kb insert at four X-linked *Om* mutants (Shrimpton et al., 1986), and is a retrovirus-like transposable element having high homology to *Drosophila melanogaster* retrotransposons *297* and *17.6* (Tanda et al., 1988). Matsubayashi et al. (1992) have examined *Om* mutants of 20 loci located on the X-chromosome and autosomes, and shown that they are all associated with the *tom* insertion, although *tom* elements also reside in other loci without discernible genetical effects.

Three *Om* loci, *Om(1D)*, *Om(2D)*, and *Om(1A)*, have so far been cloned and analyzed (Tanda et al., 1989; Tanda and Corces, 1991; Matsubayashi et al., 1991a; 1991b; Awasaki et al., 1994; Yoshida et al., 1994). In these mutants, *tom* elements insert nearby the relevant *Om* genes and activate their expressions in eye imaginal discs of third instar larvae, without affecting the structure of their products. These findings suggest that *Om* phenotypes may result from over- and/or ectopic-expression of the *Om* genes in eye imaginal discs and that a putative enhancer present within the *tom* element may be responsible for such changes (Awasaki et al., 1994; Tanda and Corces, 1991; Yoshida et al., 1994).

The products of these *Om* genes have been characterized. The *Om(1D)* and *Om(1A)* genes encode homeoproteins homologous to the *Drosophila*

melanogaster BarH1 and *cut* gene products, respectively (Kojima et al., 1991; Awasaki et al., 1994); *BarH1*, together with its sibling, *BarH2*, is required for the differentiation of R1/R6 photoreceptors and primary pigment cells in the eye imaginal disc (Higashijima et al., 1992a), as well as that of neurons and glial cells in the external sensory organ (Higashijima et al., 1992b); the *cut* gene is known to play an important role in the differentiation of the sensory mother cell into the external sensory organ (Bodmer et al., 1987; Blochlinger et al., 1988; 1991). On the other hand, the *Om(2D)* gene encodes a novel protein containing the histidine/proline repeat (PRD repeat) motif (Yoshida et al., 1994). This motif has been found in several transcription factors of Drosophila and other species, and hypothetically mediates the pH-dependent protein-protein interaction of eukaryotic transcription factors (Janknecht et al., 1991). Loss-of-function of the *Om(2D)* gene results in embryonic- or larval-lethality (Matsubayashi et al., 1991b). It is thus plausible that the *Om(2D)* gene also participates in some developmental pathways.

Based on the above findings, it is presumed that *Om* gene products may be capable of switching cell fates in given developmental pathways, and that *Om* phenotypes result from misleading of cell fates by excess *Om* gene products in differentiating eye imaginal discs. Possibility thus exists that studies of *Om* mutations may provide an approach to investigate members of such "switching genes". *Om* mutations may well have some merits to analyze: first, the transposon (i.e., *tom*)-tagging strategy facilitates cloning *Om* genes; second, the gain-of-function nature of *Om* mutations allows to identify genes which are hardly recognized with loss-of-function mutations because of lethality or redundancy [e.g., *Om(1D)* = *BarH1/H2*].

Among *Om* mutations, the *Om(1E)* mutation is quite unique because of its peculiar phenotype exhibiting overgrowth of the compound eye

without affecting the regular array of ommatidia and the ommatidial structure, while all the other *Om* mutations result in fewer-than-normal and disorganized ommatidia. Three *Om(1E)* mutant alleles, *Om(1E)53*, *Om(1E)59a*, and *Om(1E)109*, have been isolated (Hinton, 1984; Moriwaki and Tobari, 1993) and cytologically mapped to 16D on the X-chromosome (Matsubayashi et al., 1992; Shrimpton et al., 1986). In this thesis, I describe characterization of the *Om(1E)* locus. Chapter I describes external and internal phenotypes of the *Om(1E)* mutants. Chapter II deals with molecular analyses including cloning and molecular characterization of the *Om(1E)* locus, and identification of the *Om(1E)* gene. Chapter III reports the spatial expression of the *Om(1E)* gene in normal individuals. For this purpose, *in situ* hybridization and immunocytochemistry were carried out. In addition, phenotypic consequences of artificial ubiquitous over-expression of *Om(1E)* and its antisense RNA are presented.

Chapter I

Description of the *Om(1E)* phenotype

INTRODUCTION

The *Om(1E)* mutants are uniquely characterized by enlarged adult compound eyes which looks like as if one extra eye is fused dorso-posterially on another. As a first step to study the *Om(1E)* mutation, I observed external and internal phenotypes of *Om(1E)* mutants. The results showed that the ommatidial number of the mutants is 1.2- to 1.7-times as many as that of wild-type, but each ommatidium is basically normal in the mutants, that the optic lobe is enlarged, and that the *Om(1E)* phenotype appears to be caused by increasing the number of undifferentiated cells in the eye imaginal disc.

MATERIALS AND METHODS

Drosophila stocks

Drosophila ananassae stocks, *Om(1E)53*, *Om(1E)59a*, *Om(1E)109*, and their progenitor *ca*; *px*, which was used as wild-type of *Om(1E)* in this study, were provided by C. W. Hinton. All stocks were cultured at 25 °C on standard medium containing yeast, cornmeal, malt, glucose, and agar.

Scanning electron microscopy

Flies stored in 25% ethanol were dehydrated to 100% ethanol, passed through a graded series of hexamethyldisilazane (HMDS) in ethanol up to 100% HMDS, and vacuum-dried. They were then coated with gold and examined with a scanning electron microscope (Joel JSM-5400LV).

The ommatidial number per compound eye was counted on scanning electron micrographs from four female compound eyes.

Histological analyses

Flies and larvae were fixed in toto with 4% paraformaldehyde/2.5% glutaraldehyde/0.02M KH_2PO_4/0.06M Na_2HPO_4 in boiling water for 5 min and then at 4 °C for at least 2 hr. After rinse in tap water and dehydration through a series of ethanol, they were embedded in a water-miscible resin mixture containing 65% (v/v) 2-hydroxypropyl methacrylate/10% (v/v) Quetol 523/25% (v/v) methyl methacrylate/0.1% (w/v) 2,2'-azobis isobutyronitrile paste (Nisshin EM Co., Ltd.) according to the method of Kushida et al. (1985). Serial sections of about 1 μm thickness were cut with glass knives on a Sorvall MT-2 Porter-Blum ultramicrotome and stained with Giemsa solution. Three-dimensional reconstruction using computer graphics. The outlines of relevant tissues from each section were transferred to tracing paper, and the data were input into an NEC PC9801 vm computer using a digitizer. Reconstruction and volumetry were carried out using a Nikon Cosmozone 2 program.

Immunocytochemistry

Neuron-specific monoclonal antibody 22C10 (Zipursky et al., 1984) was used to visualize developing photoreceptor cells. Hand dissected brain/eye-antenna imaginal disc complexes were fixed in ethanol/acetic acid (3:1) for 30 min, then washed in PBT [0.1% Tween 20 in PBS (130 mM NaCl in 10 mM phosphate buffer, pH 7.2). The discs were treated

with PBTS (3% bovine serum albumin and 10% normal sheep serum in PBT) for 15-30 min, and with MAb22C10 in PBTS (1:200) overnight. The discs were then washed in PBT, and treated with horseradish peroxidase-linked sheep anti-mouse Ig antibody $F(ab')_2$ fragment (Amersham) in PBTS (1:200) for 2 hr. After several washes in PBT, the peroxidase label was visualized by incubation in 0.5 mg/ml diaminobenzidine, 0.03% $CoCl_2$, and 0.03% H_2O_2 in PBT.

Labeling and detection of mitotically-active cells were according to Truman and Bate (1988); hand-dissected brain/eye-antenna imaginal disc complexes were labeled *in vitro* with 5-bromodeoxyuridine in Schneider's medium (GIBCO) for 1 hr at room temperature.

The specimens were washed in PBT, mounted in Aquatex (Merck) and examined using Nomarski optics.

RESULTS

External and internal phenotypes of the *Om(1E)* mutant flies

Three *Om(1E)* mutants, *Om(1E)53*, *Om(1E)59a*, and *Om(1E)109* (Hinton, 1984; Moriwaki and Tobari, 1993) are all characterized by dorso-posteriorly enlarged compound eyes which look like as if one extra eye is fused dorso-posterially on another (Figure 1). The average number of ommatidia per compound eye is 1,353.3±90.2 in *Om(1E)53*, 1058.3±67.5 in *Om(1E)59a*, and 945.3±71.8 in *Om(1E)109*, in contrast to 816.8±34.9 in wild-type. The arrangement of ommatidia is basically normal in the mutants.

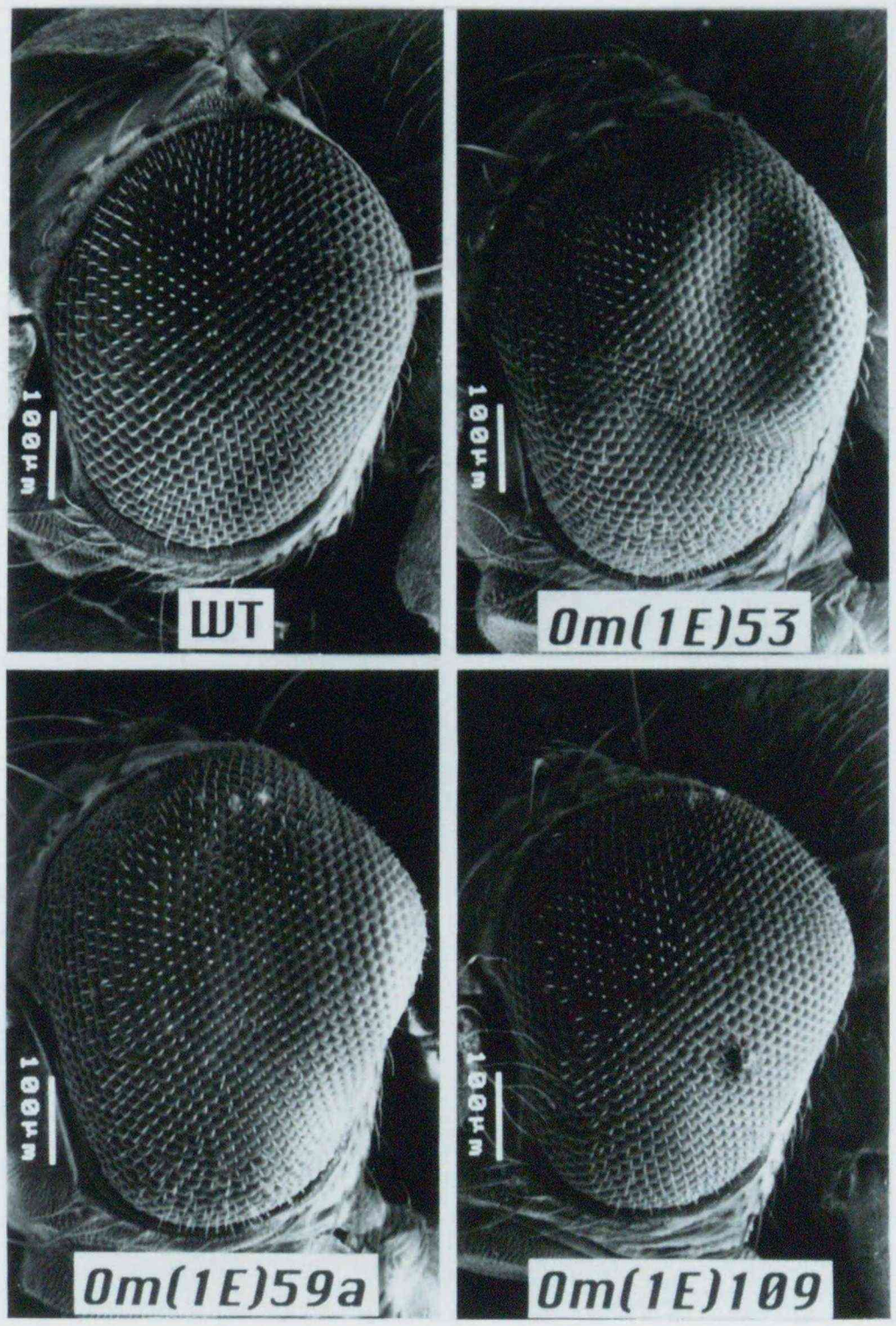

Figure 1. Scanning electron micrographs showing left compound eyes of wild-type (WT) and *Om(1E)* mutant female flies. Anterior is to the left.

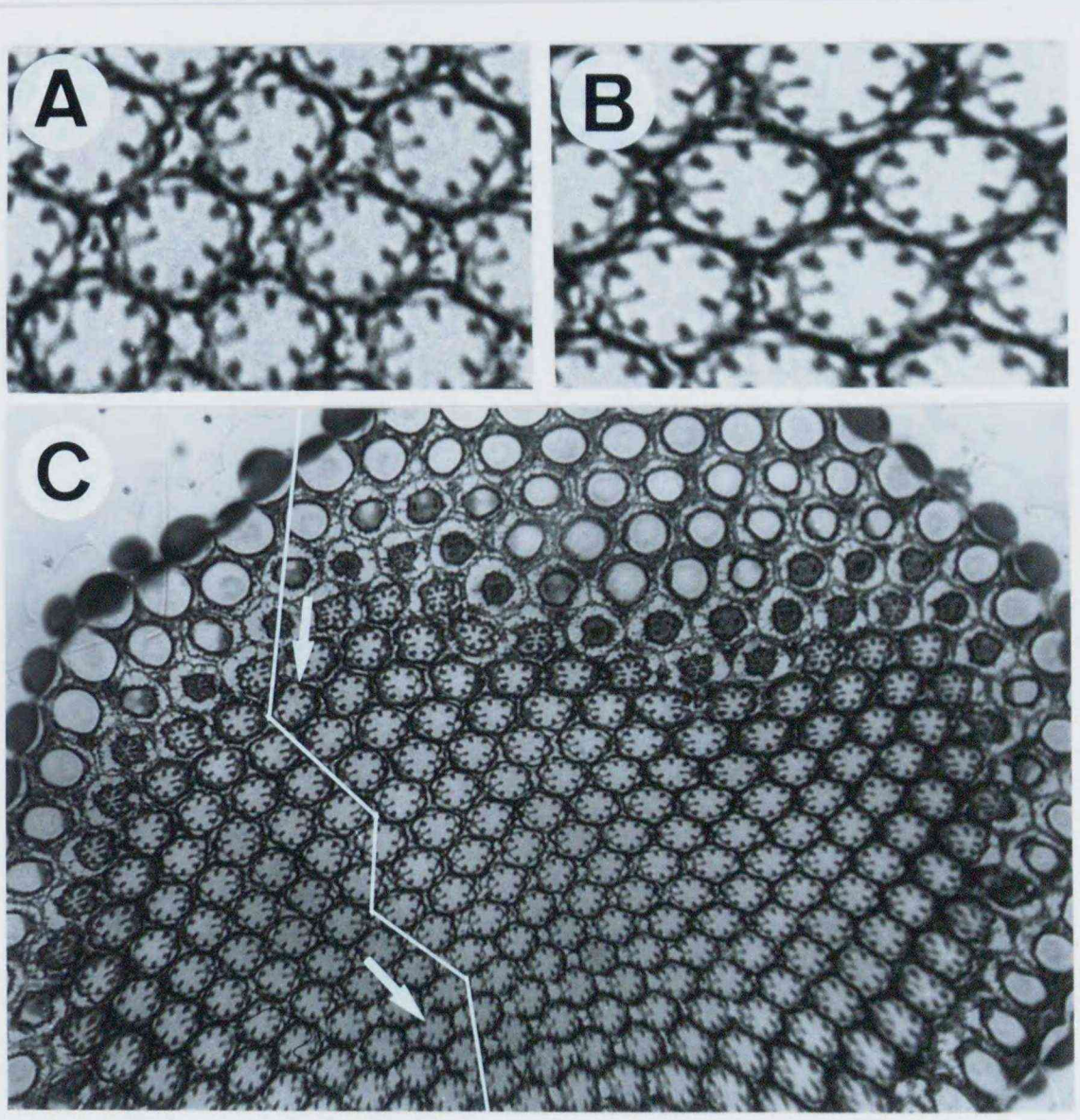

Figure 2. Tangential sections of compound eyes. (A) wild-type. In each ommatidium, the rhabdomeres of seven photoreceptor cells arranged in an asymmetrical trapezoid pattern are visible. The rhabdomere of eighth photoreceptor cell is beneath the seventh. (B) *Om(1E)53*. Note that the regular ommatidial pattern is not changed in the mutant. (C) Low magnification. The polarity is disturbed in some ommatidia (arrow) around the mirror image symmetry line which appears to be at the boundary of two overlapping eyes (line) in the *Om(1E)* mutant.

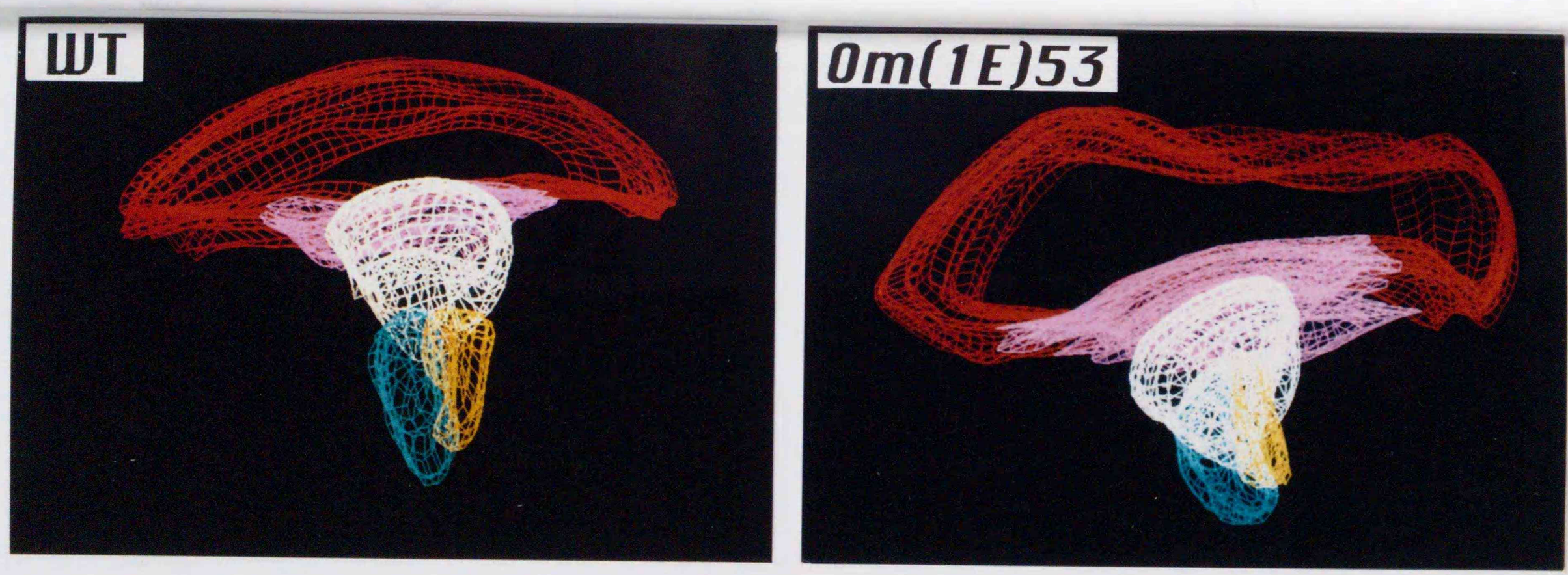

Optic lobe Volumes (x10^6 μm^3)

	wild type	*Om(1E)53*
Retina (red)	—	—
Lamina (pink)	3.65 ±0.30	5.44 ±0.14
Medulla (white)	3.48 ±0.25	5.03 ±0.26
Lobula (blue)	1.25 ±0.12	1.71 ±0.11
Lobula plate (yellow)	0.49 ±0.10	0.72 ±0.06

Figure 3. Computer-aided reconstruction and volumetry of the optic lobe. (Upper) Computer graphic reconstructions of the right optic lobes of wild-type and *Om(1E)53* (viewed from the dorsal side). Red wire shows the outline of part of compound eye. Pink, white, blue and yellow wires show lamina, medulla, lobula, and lobula plate, respectively. Anterior is to the left. (Lower) Volumes of optic lobe components are calculated using the reconstruction images.

The normal ommatidium of Drosophila consists of eight photoreceptor cells arranged in an asymmetrical trapezoid pattern, four cone cells, six pigment cells and a hair system (Figure 2; for a review, see Dickson and Hafen, 1993). The arrangement of the photoreceptor cells within the ommatidium differs in the dorsal and ventral half of the eye, and there is a mirror-image inversion of the photoreceptor cell arrangement in the middle of the eye, approximately at the level of the topographical equator (for a review, see Wolff and Ready, 1993). Such pattern formation of each ommatidium is also normal in *Om(1E)* mutants, except that the polarity is disturbed in some ommatidia around the mirror image symmetry line which appears to be at the boundary of two overlapping eyes (Figure 2), and that the ommatidial bundles are not tightly packed in the inside of the eye (data not shown).

The structure and arrangement of the optic lobe components are normal, aside from the apparent increase in their volume (Figure 3).

No other visible change was noted in the mutant.

Development of the eye imaginal disc in *Om(1E)* mutant larvae

The eye imaginal disc of Drosophila originates from a few embryonic cells. As development proceeds, undifferentiated cells in the eye imaginal disc proliferate up to about 2,000 by the third larval instar stage. The differentiation of the compound eye begins during that stage with the appearance of clusters containing photoreceptor precursors in the region posterior to the morphogenetic furrow, which sweeps from posterior to anterior across the eye imaginal disc, while undifferentiated cells still continue to proliferate in the region anterior to the morphogenetic

furrow. Each of the clusters finally differentiate into the ommatidium (for a review, see Wolff and Ready, 1993).

The histological study showed that the eye imaginal discs of *Om(1E)* mutants are normal both in size and morphology to early third larval instar stage; but during the middle and late third larval instar stages, each disc epithelium overgrows to form a bud which might later become a dorso-posteriorly protruded portion of the compound eye (data not shown). This suggests that the *Om(1E)* phenotype may result from over-proliferation of undifferentiated cells, but not from over-production of photoreceptor clusters at the expense of cells which are normally not involved in the cluster formation. This was tested in the present study by immunostaining with neuron specific antibodies, MAb22C10 which enables to visualize photoreceptor precursors (Zipursky et al., 1984). In the wild-type eye imaginal disc, single photoreceptor precursors (R8) are seen immediately posterior to the morphogenetic furrow with clusters of three to five photoreceptor precursors in the farther posterior region, all being regularly arranged (Figures 4A and 4C; for a review, see Wolff and Ready, 1993). Such regular arrangement and density of the clusters does not seem to be affected in *Om(1E)* mutants (Figures 4B and 4D). This is in agreement with the above suggestion. However, 5-bromodeoxyuridine (BrdU)-labeling assays failed to demonstrate that the mutant eye imaginal discs are more mitotically active than the wild; no difference of mitotic activity was observed between wild-type and mutant flies (Figures 4E and 4F). As mentioned earlier, the number of ommatidia per compound eye in the three allelic mutants is not greater than twice the number in wild-type. This means that the mitotic frequency in the mutant eye imaginal discs need not be doubled, thus the change of the mitotic rate may be, if any, hard to be detected by the method employed.

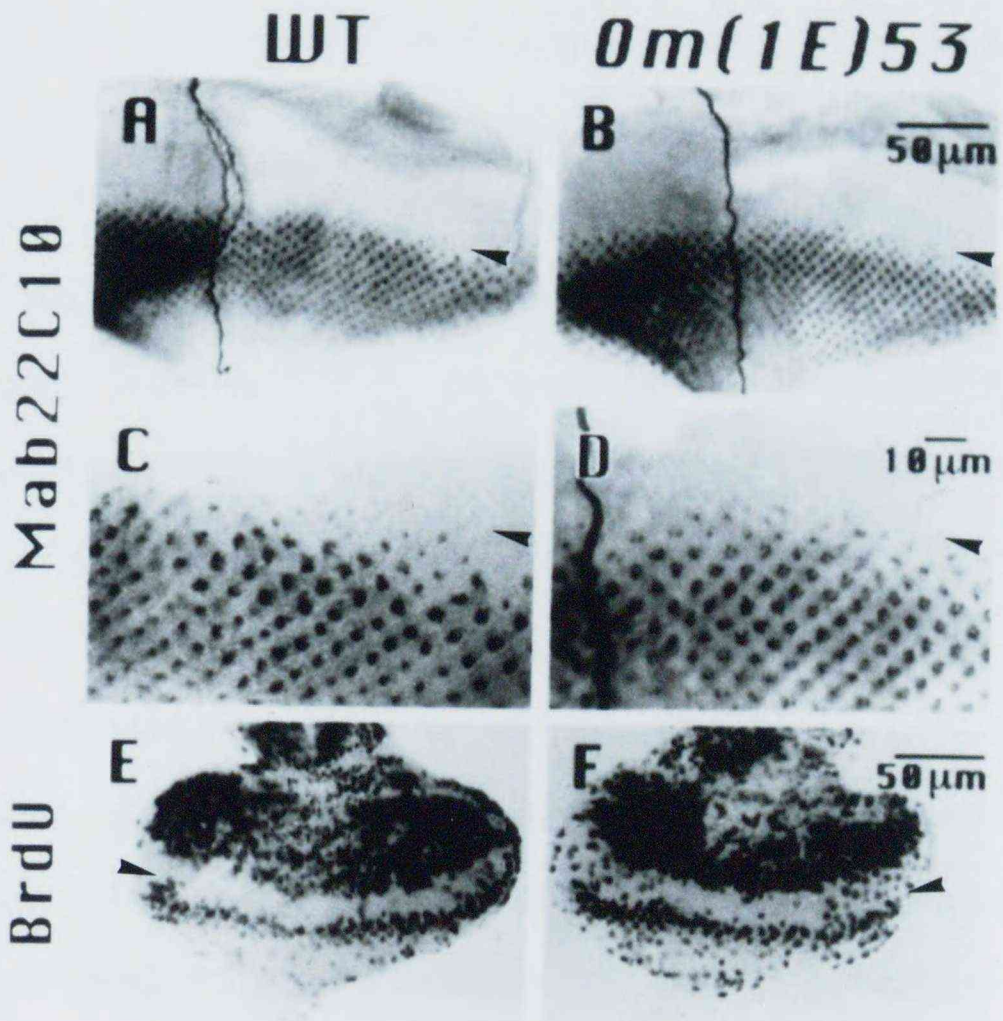

Figure 4. Whole mount eye imaginal discs from third instar larvae of wild-type (left) and *Om(1E)53* (right). (A and B) Eye imaginal discs stained with MAb22C10 highlighting photoreceptor precursor cells. (C and D) Higher magnifications of A and B, respectively, showing regions immediately posterior to the morphogenetic furrow. Note that the array of photoreceptor precursor clusters is normal in the mutant. (E and F) BrdU-labeling highlighting mitotically-active cells. Arrowheads mark positions of the morphogenetic furrow. Anterior is to the top.

DISCUSSION

The phenotype of the *Om(1E)* mutants exhibits overgrowth of the compound eye with surplus, normally-patterned ommatidia. The observation of developing eye imaginal discs has suggested that the overgrowth of the mutant compound eye may result from over-proliferation of undifferentiated cells in the eye imaginal disc. No such phenotype has been seen in other *Drosophila ananassae* mutants (Moriwaki and Tobari, 1993) as well as in *Drosophila melanogaster* mutants reported so far (Lindsley and Zimm, 1992).

In addition to increase of ommatidial number, the *Om(1E)* mutants also exhibit overgrowth of the optic lobe. This is also in contrast to other *Om* mutants which display atrophy of the optic lobe (Tanda et al., 1993). However, these optic lobe abnormalities may not be primary effects of the *Om* mutations. In *Om* mutants so far analyzed (Awasaki et al., 1994; Tanda and Corces, 1991; Yoshida et al., 1994) as well as in the *Om(1E)* mutants (see Chapter II), the relevant *Om* genes are over-expressed in the eye imaginal disc resulting in abnormal eye development, but not in optic lobe primordia. It is thus unlikely that mutated *Om* genes *per se* affect the optic lobe development.

It is known that the development of the optic lobe generally depends on innervation of the photoreceptor axons, while the compound eye development is autonomous. Genetic mosaic analyses have demonstrated that the optic lobe, irrespective of its genotype, fails to differentiate whenever the eye imaginal disc is photoreceptor-deficient mutants. (for a review, see Meinertzhagen and Hanson, 1993). It is therefore likely that the overgrowth or atrophy of the optic lobe in *Om* mutants are the consequence of increase or decrease of photoreceptor neurons, respectively.

Chapter II

Molecular genetics of the *Om(1E)* locus

INTRODUCTION

In order to characterize the *Om(1E)* mutation and the *Om(1E)* gene, molecular analyses of the *Om(1E)* locus were carried out. Since the *Om(1E)* mutation has been suggested to be caused by insertion of the *tom* element (Shrimpton et al., 1986; Matsubayashi et al., 1992), I employed a transposon-tagging strategy (Bingham et al., 1982) and chromosomal walking (Bender et al., 1983), and cloned a putative *Om(1E)* region of 70-kb long. Of two transcribed regions found in the vicinity of *tom* insertion sites of the three *Om(1E)* mutant alleles, one was shown to be the *Om(1E)* gene by analyses of gene expression patterns in wild-type and mutant eye imaginal discs, and by *P*-element-mediated transformation with *Drosophila melanogaster*. The deduced *Om(1E)* gene product is a novel protein having presumptive transmembrane domain(s).

MATERIALS AND METHODS

Drosophila stocks

Drosophila ananassae stocks, *Om(1E)53*, *Om(1E)59a*, *Om(1E)109*, and their progenitor *ca*; *px*, which was used as wild-type of *Om(1E)* in this study, were provided by C. W. Hinton. Revertants of *Om(1E)53*, $Om(1E)53^{R1}$ and $Om(1E)53^{R2}$ were isolated from 8,762 X-chromosomes of *Om(1E)53* males which had been irradiated with 30 Gy of γ-ray from a ^{60}Co source. These revertants are viable and fertile, and maintained in males by crossing to C(1LR)*f g*/Y females (Y. N. Tobari, personal communication). The D38 strain was provided by Y. N. Tobari. The *Drosophila melanogaster w* strain was obtained from National Institute of

Genetics, Mishima, Japan. All stocks were cultured at 25 °C on standard medium containing yeast, cornmeal, malt, glucose, and agar.

Molecular techniques

Routine molecular techniques were according to Sambrook et al. (1989).

Analyses of genomic DNA

Preparation of genomic DNA was after Itoh et al. (1988). Genomic libraries were constructed with Sau3AI partially-digested genomic DNAs and the λEMBL3 vector. The *tom* probe, ptom1, is a 6.5-kb SacI fragment of λ63-13 (Matsubayashi et al., 1991a) which contains all of the *tom* sequences except for one of the two LTRs. Library screening and Southern hybridization were performed using digoxigenin-labeled probes and the DIG Luminescent Detection Kit (Boehringer Mannheim) according to the manufacture's instruction.

in situ hybridization to polytene chromosomes was performed using digoxigenin-labeled probes and the DIG DNA Detection Kit (Boehringer Mannheim), following the method of Engels et al. (1986).

RNA isolation and Northern blot analysis

Total RNAs were extracted by the hot phenol method (Jowett, 1986), and polyA$^+$ RNAs were prepared using the mRNA purification kit

(Pharmacia). PolyA$^+$ RNAs (3 μg/lane) were separated on formaldehyde-denatured 1% agarose gels, blotted onto the Biodyne-A nylon membrane (Paul), and hybridized with ^{32}P-labeled probes prepared with the Multiprime DNA labeling system (Amersham). As a control for the amount of RNA loaded in each lane, the blots were rehybridized with a *Drosophila melanogaster ras2* gene probe, pUC8-HB-1.2kb (Bishop and Corces, 1988), which was provided by V. G. Corces.

Cloning and sequencing of cDNAs

A cDNA library was constructed as described by Yoshida et al. (1994) with oligo-dT primed cDNAs of the wild-type third instar larvae and the λgt10 vector. The cDNA library was screened by the same method as for genomic library screening. The retrieved cDNAs were recloned in the pGEM7zf(-) plasmid vector (Promega). Nucleotide sequences were determined by the chain-terminating method (Sanger et al., 1977) using the BcaBest Dideoxy Sequencing Kit (Takara) and sequential deletion mutants (Henikoff, 1984).

***in situ* hybridization to whole mount eye imaginal discs**

Hand-dissected tissues were fixed in 4% paraformaldehyde in PBS [130 mM NaCl in 10 mM phosphate buffer (pH 7.2)] on ice for 15 min, and then in 4% paraformaldehyde and 0.5% Triton-X 100 in PBS at room temperature for 15 min. Pre-treatment, hybridization and signal-detection were made as described by Tautz and Pfeifle (1989) except that antisense RNA probes were used instead of double stranded DNA probes.

Digoxigenin-labeled RNA probes were synthesized from cDNAs cloned in the pGEM7zf(-) vector using the DIG RNA Labeling Kit (Boehringer Mannheim) according to the manufacture's instruction; the labeled RNAs were size-reduced to the average length of 50-100 bases by controlled alkaline hydrolysis to achieve the efficient hybridization (Cox et al., 1984). At the beginning and the end of the washing step after hybridization, the specimens were treated with 20 μg/ml RNaseA and 0.5 M NaCl in 10 mM Tris buffer (pH 8.0) at 37 °C for 30 min to remove the unhybridized probe. After signal-detection, the specimens were washed in 0.1% Tween 20 in PBS, and mounted in Aquatex (Merck).

_P_-element mediated transformation

A 0.3-kb SalI-PstI fragment spanning -0.2 to +0.1 kb from the initiation site of the *Hsp70* gene was excised from phsp70C4 (Tanda and Corces, 1991), and cloned in the XbaI site of the CaSpeR vector (Pirrotta et al., 1985) so as to orient the *Hsp70* promoter parallel to the w^+ marker gene. This construct was named HspCaSpeR1. Furthermore, an EcoNI-TaqI fragment ranging nucleotides -13-434 of the 3' *tom* LTR was excised from λ63-13 (Matsubayashi et al., 1991a), and cloned in the PstI site of the HspCaSpeR1 vector in the opposite direction to the *Hsp70* promoter. This was named TLHspCaSpeR. The t1 and t2 cDNAs (see RESULTS) flanked by EcoRI linkers were cloned in each of HspCaSpeR1 (Hsp-t1/t2 constructs) and TLHspCaSpeR (TLHsp-t1/t2 constructs) at the EcoRI site downsteam the *Hsp70* promoter (see Figure 5). Since the t1 cDNA lacked for 0.5 kb of the 3' untranslated region containing the polyadenylation signal, its genomic counterpart was fused to the t1 cDNA before introducing into the vectors. The resulting constructs were co-injected

with pπ25.7wc (Karess and Rubin, 1984) into embryos of the *Drosophila melanogaster w* strain by the method of Rubin and Spradling (1982). Transformants were selected from the G_1 flies and individually crossed to *w* flies. Homozygous transformant lines were established by single-paired sib-mating for further two or more generations.

Scanning electron microscopy

Scanning electron microscopy was made as described in Chapter I. The average ommatidial number per compound eye was counted on scanning electron micrographs from four female compound eyes.

RESULTS

Cytological locations of *tom* inserts in *Om(1E)* mutants

Based on examination of the *Om(1E) 53* mutant, it has been reported that the *Om(1E)* mutation is associated with the *tom* insertion cytologically mapped to 16D on the right arm of X-chromosome (Matsubayashi et al, 1992; also designated 14C on Hinton's map, Shrimpton et al., 1986). Prior to molecular cloning of the *Om(1E)* locus, I reexamined *tom*-insertion sites on polytene chromosomes of *Om(1E)* mutants including *Om(1E)53*, *Om(1E)59a*, and *Om(1E)109* by *in situ* hybridization using the ptom1 as a probe. The results revealed that all three *Om(1E)* mutants indeed have the *tom* insert at 16D (Figure 1A, 1B,

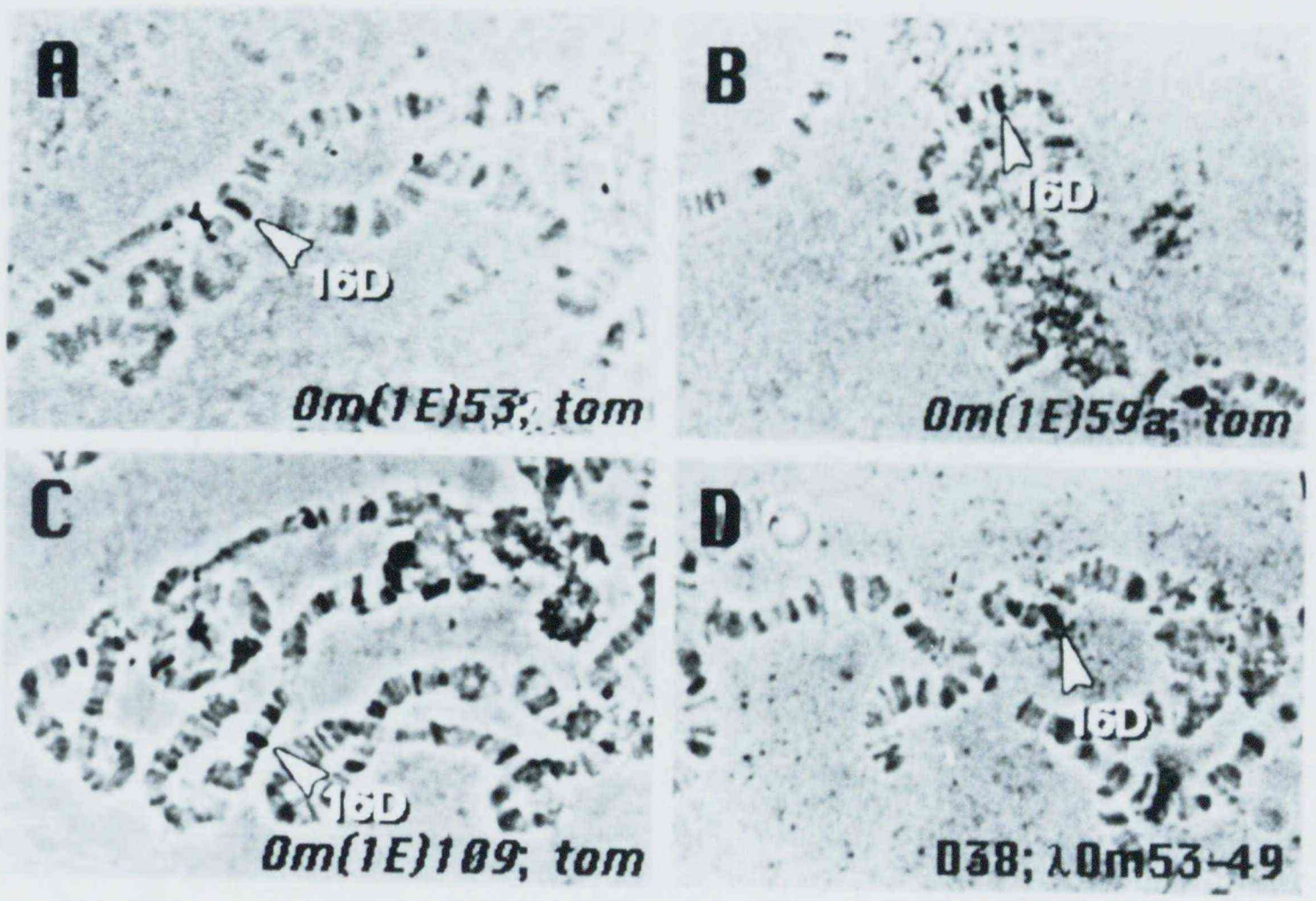

Figure 1. *in situ* hybridization of polytene chromosomes. (A-C) Polytene chromosomes of the *Om(1E)* mutants hybridized with a *tom* probe. (D) Polytene chromosome of the D38 strain hybridized with λOm53-49.

and 1C), while they have different sets of *tom*-positive loci (data not shown). The number of *tom*-positive loci is five in *Om(1E)53*, and at least ten in *Om(1E)59a* and *Om(1E)109*.

Molecular cloning and characterization of the *Om(1E)* region

To clone the *Om(1E)* locus by the *tom*-tagging strategy, I constructed a genomic library of *Om(1E)53* because of its paucity of *tom* inserts in the genome, and screened with a *tom* probe, ptom1. Since the *Om(1E)53* genome has silent *tom* elements inserted in at least four other sites, retrieved clones were mapped by *in situ* hybridization to polytene chromosomes of the D38 strain which has the *tom*-free X-chromosome (unpublished data). As a result, one of 64 retrieved clones, λOm53-49, hybridized uniquely to the 16D region (Figure 1D). With this clone, sequential chromosome walking on a wild-type (*ca; px*) genomic library was performed, and a putative *Om(1E)* region of 70 kb long was obtained (Figure 2A).

Genomic structures of the *Om(1E)* alleles were analyzed by Southern hybridization using DNA probes derived from the cloned region. As a result, 7-kb and 3-kb insertions were found in *Om(1E)59a* and *Om(1E)109*, respectively, within the HindIII 3.8-kb region about 25 kb downstream from the *tom* insertion site in *Om(1E)53* (Figure 2B-a). To characterize these inserts, I cloned λOm59a-1 and λOm59a-2 from an *Om(1E)59a* genomic library, and λOm109-1 from an *Om(1E)109* genomic library using the pHH3.8 probe which spans the insertion site (Figure 2A). Analyses of these clones by restriction mapping and Southern hybridization with the ptom1 probe revealed that the insertions are indeed *tom* elements, their directions being similar to that of the *tom*

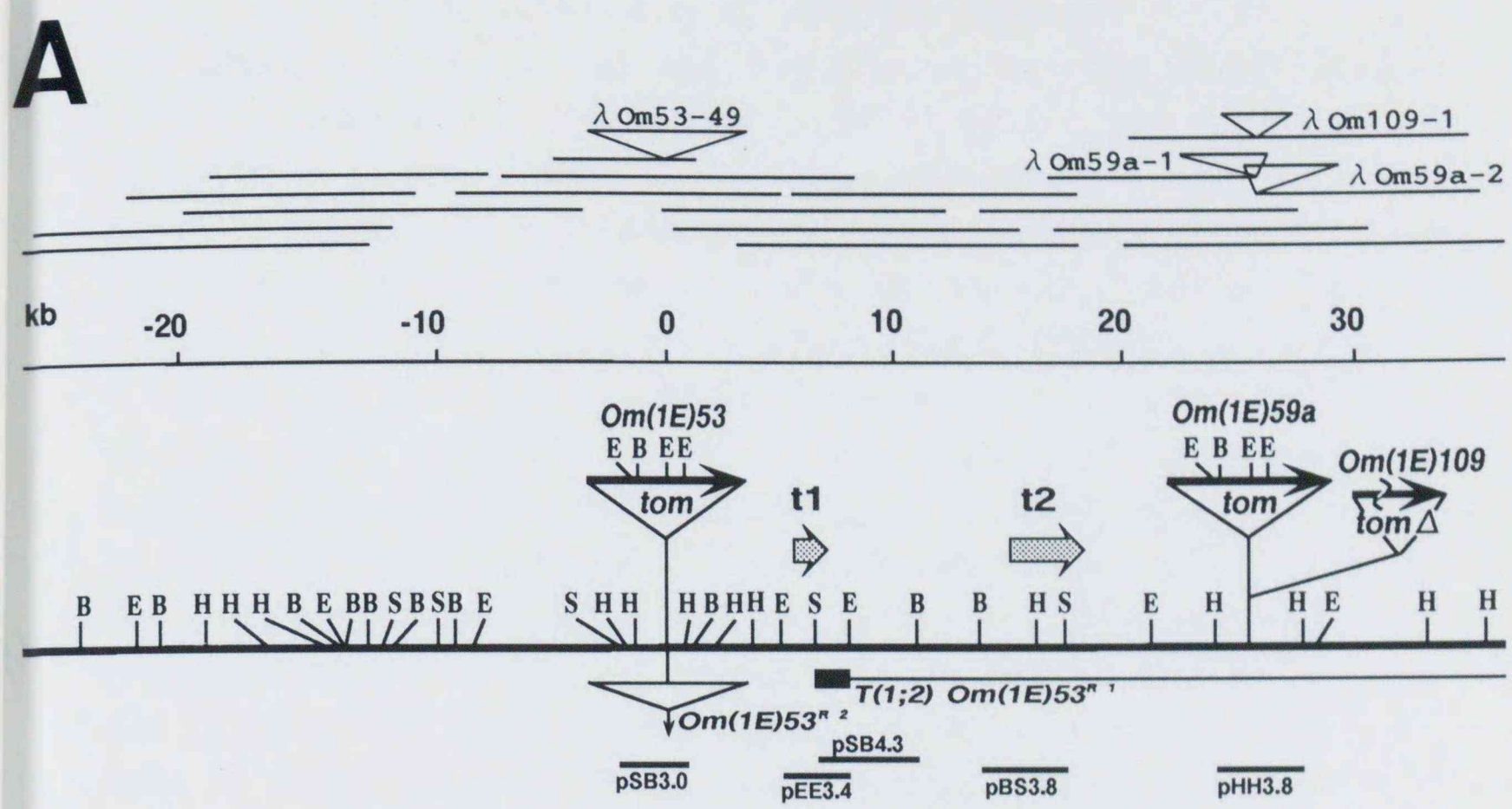

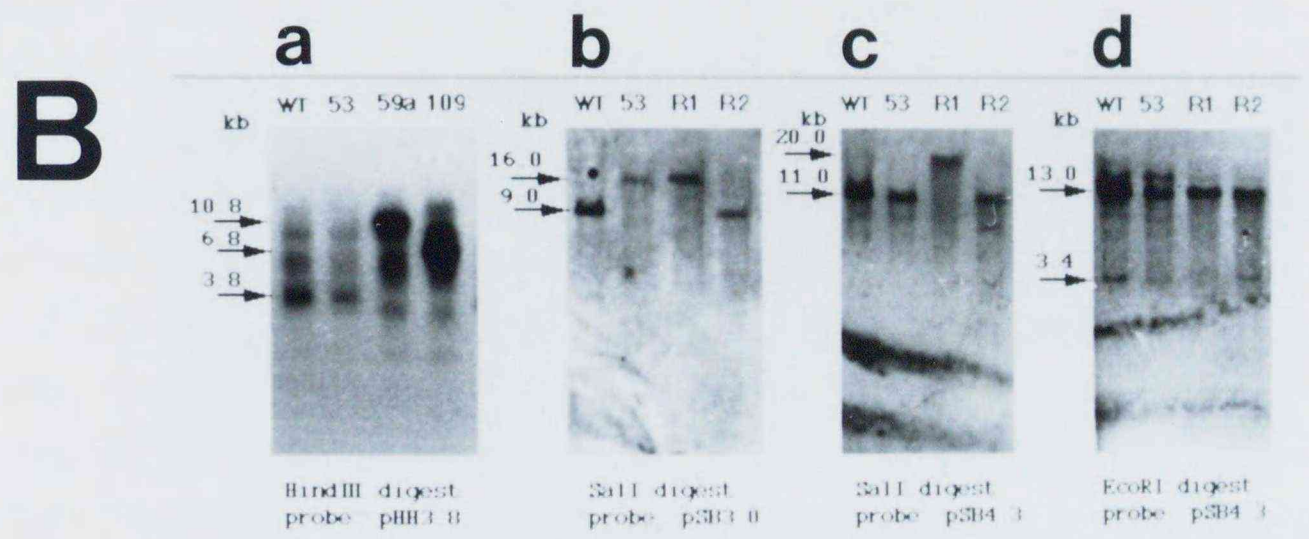

Figure 2. (*see following page for legend.*)

Figure 2. Molecular analyses of the *Om(1E)* region.
(A) Molecular structure of the *Om(1E)* region. The middle line is a restriction map of the wild-type (*ca; px*) genome. Upper and lower bars designate λ phage clones and probes, respectively. *tom* insertions in *Om(1E)* mutants are represented by solid arrows that indicate their orientations. *tom*Δ means the internally-deleted *tom* element. The region containing the breakpoint in *Om(1E)53^{R1}* [T(1;2)16D;26C] is indicated by a closed box. Potential deletion of the *tom* insertion in *Om(1E)53^{R2}* is symbolized by a triangle below the map. Positions and orientations of the transcribed regions t1 and t2 are indicated by dotted arrows. Restriction sites are B: BamHI; E: EcoRI; H: HimdIII; S: SalI.
(B) Southern blot analysis of wild-type (WT), *Om(1E)53* (53), *Om(1E)59a* (59a), *Om(1E)109* (109), and revertants of *Om(1E)53* , *Om(1E)53^{R1}* (R1) and *Om(1E)53^{R2}* (R2). Hybridization probes and restriction enzymes used to digest genomic DNAs are indicated bellow each panel. (a) A Southern blot suggesting existence of insertion in the *Om(1E)59a* and the *Om(1E)109* alleles. Note that the HindIII 3.8-kb fragment is shifted to 10.8 kb and 6.8 kb in *Om(1E)59a* and *Om(1E)109*, respectively. (b-d) Southern blots indicating alterations of DNA structure in the revertants.
(C) Northern blot analysis showing developmental expression of t1 (upper) and t2 (middle). Rehybridization with a *ras2* probe (Bishop and Corces, 1988) was performed as a control for the amount of RNA loaded in each lane (lower). Developmental stages are embryos, first-second instar larvae (1st-2nd), early (feeding) third instar larvae (early 3rd), late (wandering) third instar larvae (late 3rd), early pupae, late pupae, and adults. No structural difference was noted between the t1 and t2 transcripts of wild-type (WT) and *Om(1E)53* (53) judging from the sizes of the transcripts. In *Om(1E)53^{R1}* (R1), the t1 transcript is truncated.

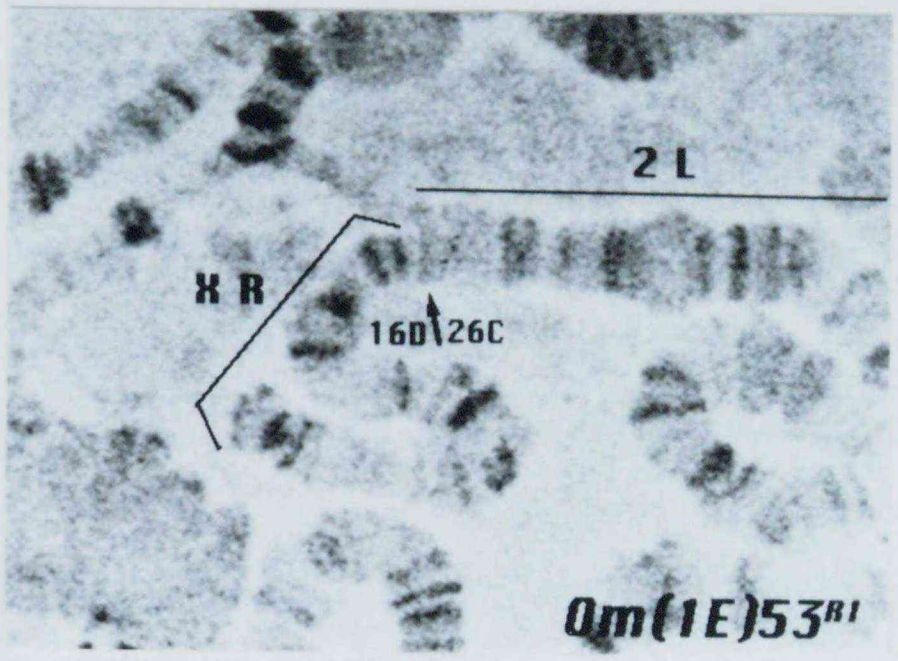

Figure 3. Polytene chromosome of the revertant *Om(1E)53^{R1}* showing the breakpoint of T(1R;2L)16D;26C.

insertion in *Om(1E)53* (data not shown). However, the *tom* element in *Om(1E)109* is defective and consists of approximately 1-kb of 5' and 2-kb of 3' ends of the intact *tom* element.

To confirm involvement of the cloned region in the *Om(1E)* mutation, I isolated and analyzed two γ-ray induced complete revertants of *Om(1E)53*; *Om(1E)53*^{R1} and *Om(1E)53*^{R2}. Southern blot analyses with the pSB4.8 probe indicate that *Om(1E)53*^{R1} has a breakpoint of a gross rearrangement within the SalI-EcoRI 1.5-kb region; the 11-kb SalI fragment shifts to 20 kb (Figure 2B-c), and the 3.4-kb EcoRI fragment is absent, while the 13-kb EcoRI fragment is intact (Figure 2B-d). In agreement with this, cytological observation of polytene chromosomes found that the rearrangement is T(1R;2L)16D;26C (Figure 3). On the other hand, *Om(1E)53*^{R2} seems to have resulted from loss of the inserted *tom* element, since the SalI fragment detected with the pSB3.0 probe is similar in length as that of wild-type (Figure 2B-b). Complete loss of inserted *tom* elements has often been seen in complete revertants of *Om* mutations (Tanda et al., 1989; Matsubayashi et al., 1991a; Awasaki et al., 1994). These results imply that the cloned region and the *tom* insertions therein may be responsible for the *Om(1E)* mutation.

Transcribed regions within the *Om(1E)* locus

I surveyed transcribed regions by Northern blot analyses using various DNA fragments spanning all over the cloned region as probes. As a result, two transcribed regions, t1 and t2, were identified between the *tom* insertion site of *Om(1E)53* and that of *Om(1E)59a* or *Om(1E)109* (Figure 2A). The t1 region expresses a 1.8-kb transcript throughout development except for the embryonic stage, whereas t2 encodes a 2.6-kb transcript

which is expressed in embryos, late third instar larvae, pupae and adults (Figure 2C). No structural difference was noted between the t1 or t2 transcripts of wild-type and *Om(1E)53* judging from their sizes. In $Om(1E)53^{R1}$, the t1 transcript seems to be truncated to 1.3 kb (Figure 2C).

For further analyses, I screened a third larval instar cDNA library of wild-type with pEE3.4 and pBS3.8 as probes, and obtained cDNA clones derived from t1 and t2, respectively. Approximate positions and orientations of the t1 and t2 transcribed regions, shown in Figure 2A, were determined from their cDNA sequences (see below) and partial genomic sequences (data not shown).

Expression of t1 and t2 RNAs in developing eye imaginal discs

The t1 and t2 transcripts were localized by *in situ* hybridization to whole mount eye imaginal discs using antisense RNA probes synthesized from the t1 and t2 cDNAs. In wild-type eye imaginal discs, t1 is expressed in a narrow region corresponding to the morphogenetic furrow at the late third larval instar stage (Figure 4A-c), is not detected at the early third instar stage (Figure 4A-a), whereas t2 expression is almost at the background level throughout the third larval instar stage (Figures 4B-a and 4B-c). In eye imaginal discs of *Om(1E)53*, both t1 and t2 are over-expressed in a similar fashion: their expression is seen in the posterior region of the eye imaginal disc in early third instar larvae where no morphogenetic furrow is seen (Figures 4A-b and 4B-b), whereas in the late third instar stage, the region of expression is around the morphogenetic furrow then locating in the center of the eye imaginal disc (Figures 4A-d and 4B-d). Such an activation of the gene expression is

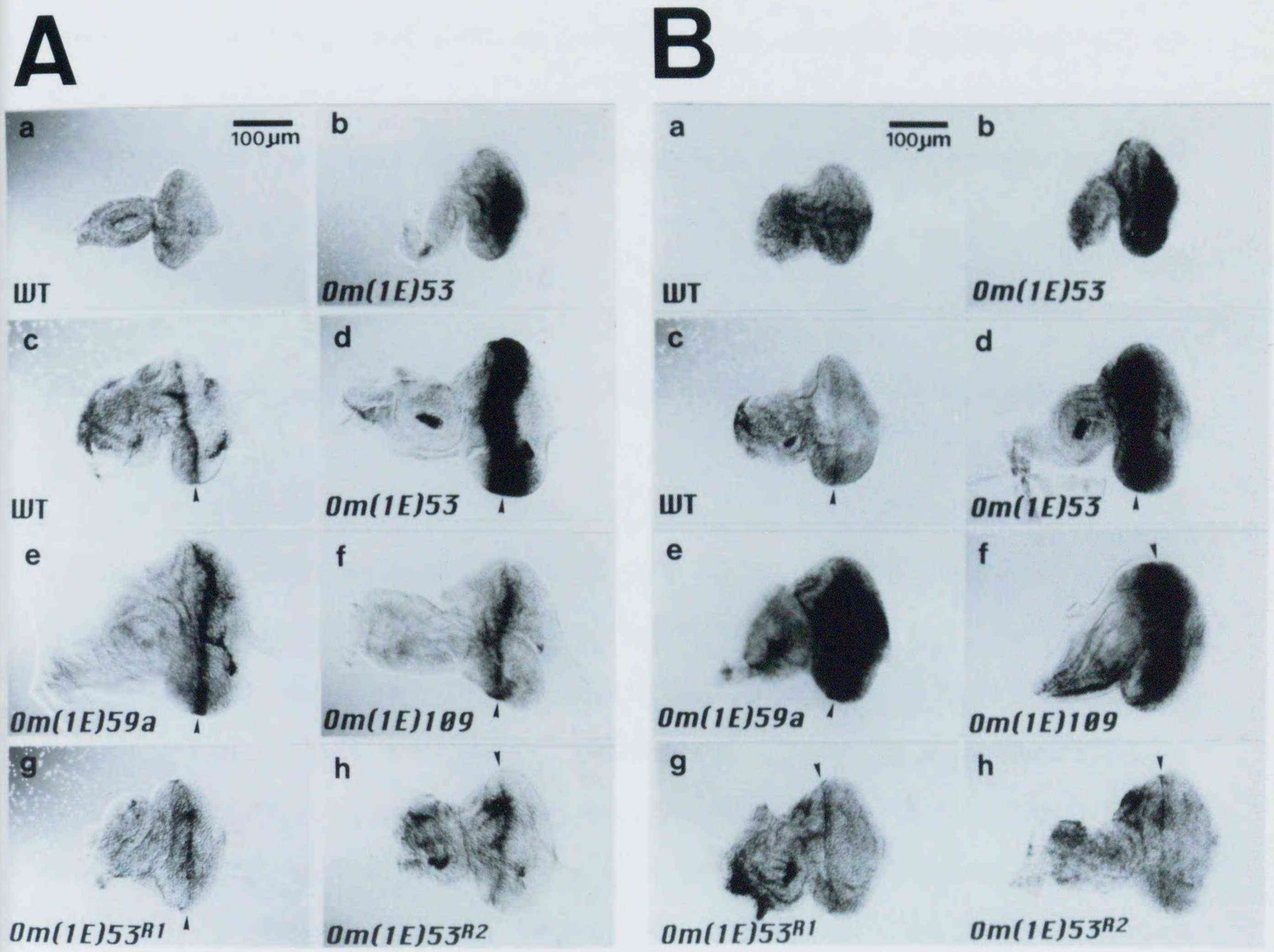

Figure 4. In situ hybridization to t1 and t2 RNAs in whole mount eye imaginal discs.

(A and B) Expression of t1 (A) and t2 (B) transcripts in eye imaginal discs of wild-type (WT), *Om(1E)* mutants, and revertants. In both panels, a and b are early third instar larval eye imaginal discs in which the morphogenetic furrow is not yet present, and c-h are late third instar larval eye imaginal discs. All eye imaginal discs are of female except for revertants. Positions of the furrow is marked by arrowheads.

not seen in *Om(1E)53*^{R1} and *Om(1E)53*^{R2} (Figures 4A-g, 4A-h, 4B-g, and 4B-h). This indicates that the activated expression of t1 and t2 in *Om(1E)53* is driven by the *tom* insertion. Eye imaginal discs of *Om(1E)59a* and *Om(1E)109* also display intense t2 expression as in *Om(1E)53* (Figures 4B-e and 4B-f), but they are not distinguishable from wild-type eye imaginal discs with respect to the t1 expression (Figures 4A-e and 4A-f).

Hsp70 promoter-t2 transformants mimics the _Om(1E)_ phenotype

To determine which region is the *Om(1E)* gene, *Drosophila melanogaster* flies were transformed with either t1 or t2 cDNA, and their effects were studied. There are two ways for inducing the expression of the t1 and t2 cDNA: one is heat-induction using *Hsp70* promoter-cDNA fusion genes (Hsp-t1 and Hsp-t2 constructs, Figure 5), and the other is *tom* LTR-driven expression using constructs of *Hsp70* promoter-cDNA plus *tom* LTR which presumably carries a transcriptional enhancer. Preliminary transformation experiments with a *tom* LTR-minimal promoter-*lacZ* reporter gene construct have shown that the *tom* LTR is a potential driver of gene expression in the eye imaginal disc. A DNA fragment containing nucleotides -13-434 of the 3' *tom* LTR was therefore placed upstream of Hsp-t1/t2 constructs in the opposite direction to prevent transcription starting from the *tom* promoter (TLHsp-t1 and TLHsp-t2 constructs, Figure 5). Using the *P*-element-mediated transformation technique (Rubin and Spradling, 1982), I established one Hsp-t1, six TLHsp-t1, one Hsp-t2 and five TLHsp-t2 transformant lines. Analyses of these transformants demonstrated that the t2 cDNA can evoke overgrowth of the compound eye (see below), while none of the

Hsp-t1 nor TLHsp-t1 transformants exhibit any morphological change (data not shown).

As compared with the *white* (*w*) strain (Figures 6A-a and 6C), about 17% increase of ommatidial number was observed in Hsp-t2 transformants without heat-induction (Figures 6A-b and 6C). This seems to be due to leaky expression at a low level, since whole mount *in situ* hybridization shows that the t2 expression in eye imaginal discs of Hsp-t2 transformants without heat-induction is as weak as that of the *w* strain (Figure 6B). On the other hand, about 40% increase of ommatidia was observed in Hsp-t2 transformants which had been subjected to three 1-hr heat-inductions at 37 °C at 2-hr intervals during the early (feeding) third instar stage (Figures 6A-c and 6C). When the transformants received the same treatment during the late (wandering) third larval instar stage, the increase of ommatidia was less prominent, being about 27% (Figure 6C). In addition to overgrowth of the compound eye, heat-induced ubiquitous over-expression of t2 during the third larval instar period evoked aberrations of wing imaginal disc derivatives very often (see Chapter III).

It is noteworthy that the ommatidial numbers of the five independent TLHsp-t2 transformants (#1-#5) were always greater than those of the Hsp-t2 transformant when not treated with heat (27-55% increase, Figures 6A-d and 6C). No other morphological change was observed. This suggests eye imaginal disc specific enhancement of gene expression by the *tom* LTR. Whole mount *in situ* hybridization confirmed that the t2 expression was intensely induced in eye imaginal discs of third instar larvae of TLHsp-t2 transformants, while no obvious t2 expression was seen in eye imaginal discs of *w* and Hsp-t2 larvae received no heat-treatment (Figure 6B). These results demonstrate that t2 is the *Om(1E)* gene, and that the *tom* LTR may have an tissue-specific enhancer function.

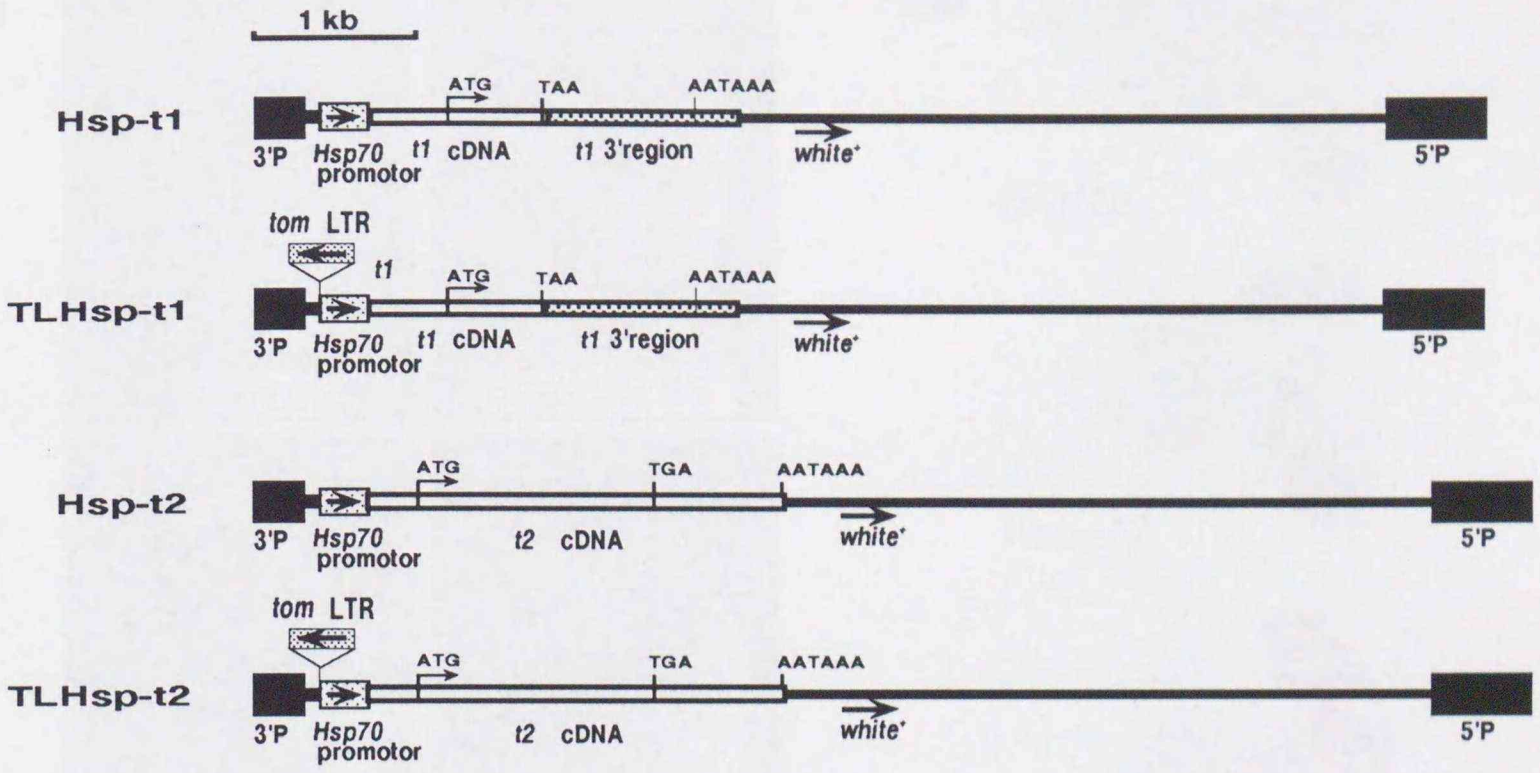

Figure 5. Schematic representation of gene constructs used for *P*-element-mediated transformation.

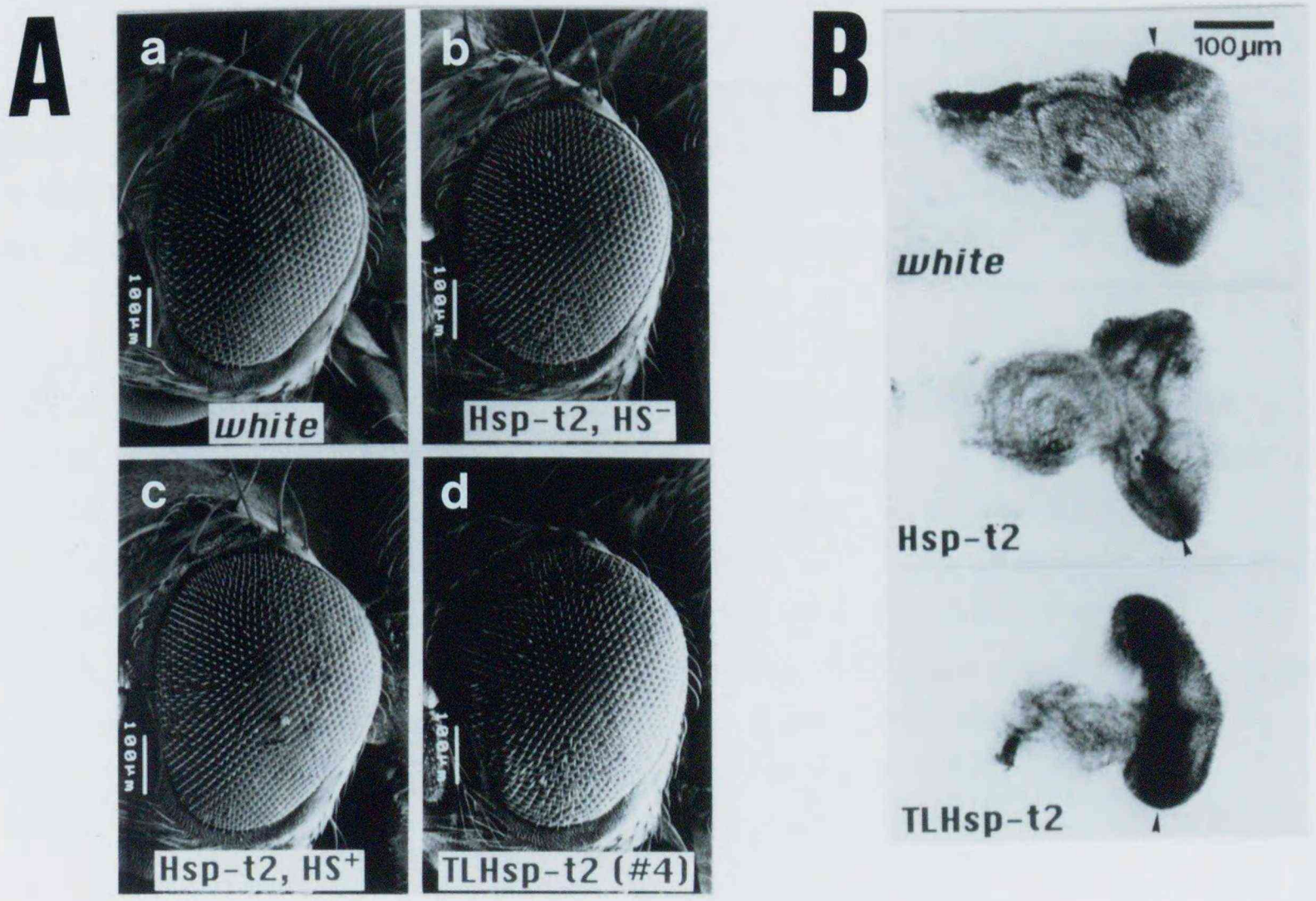

Figure 6. (*see following page for legend.*)

Figure 6. (A) Scanning electron micrographs showing female left compound eyes of *white*, and transformants carrying t2 cDNA constructs. Anterior is to the left. (a) *white*; (b) Hsp-t2 transformant received no heat-induction; (c) Hsp-t2 transformant received heat-induction during the early third instar stage; (d) an example of TLHsp-t2 transformants (line #4) received no heat-induction.
(B) Showing t2 expression in whole mount eye imaginal discs of *white* (upper), Hsp-t2 transformant (middle), and TLHsp-t2 transformant (line #2) (lower). All eye imaginal discs were prepared from female late third instar larvae which received no heat-induction. Arrowheads indicate positions of the morphogenetic furrow. Anterior is to the left.
(C) Average ommatidial numbers of female left eyes of *white* (*w*), Hsp-t2 and five independent TLHsp-t2 transformant lines (#1-#5). Hsp-t2 transformants were raised without heat-induction (no), and heat-induction during the early third instar stage (@E3rd) or the late third instar stage (@L3rd). N=4. Bars indicate standard deviations.

cDNA sequence and deduced protein of *Om(1E)*

Figure 7 shows the nucleotide sequence of the *Om(1E)* cDNA and the deduced polypeptide sequence. The *Om(1E)* cDNA consists of 2,597 bp in agreement with the mRNA length predicted from the Northern blot analysis. Potential polyadenylation signals (AATAAA) are at the nucleotide positions 2541 and 2553, followed by the poly(A) tail starting at the nucleotide position 2584. There are six repeats of RNA instability motif (ATTTA; Shaw and Kamen, 1986) within the putative 3' untranslated region, suggesting rapid turnover of this message. The cDNA contains a potential open reading frame (ORF) of 1,590 nucleotides starting from the first methionine codon at the nucleotide position 311. The deduced protein is 530 residues long with the predicted molecular mass of 59 kDa. However, if started from the second methionine codon at the nucleotide position 509, the protein product may be 464 residues long with the predicted molecular mass of 53 kDa. Although these potential translation start sites do not match the typical translation start consensus of Drosophila (C/AAC/AATG; Cavener, 1987), the protein would start at one of these sites, because anti-Om(1E) antibodies detect about 55 kDa protein on a Western blot (see Chapter III).

The overall sequence of the *Om(1E)* cDNA and the deduced protein have no significant homology with any other sequences registered in the DDBJ/GenBank/EMBL databases and the SWISS-PLOT protein database. The amino acid content of the deduced protein is rich in serine, arginine, and glutamine (about 10% residues each). The protein has a poly-serine stretch (residues 125-151) following a threonine-rich stretch (residues 89-122), and a glutamine-rich stretch (residues 432-466). As shown by the GES-scaled hydrophobicity plot in Figure 8 (Engelman et al., 1986), the deduced protein is hydrophilic as a whole, having three

large peaks of basic cluster (residues 154-162, 192-202 and 428-467). The last peak and the glutamine-rich stretch constitute a large hydrophilic domain in the carboxyl terminus (residues 428-467). In addition to these hydrophilic domains, there are two prominent hydrophobic domains (residues 62-82 and 117-137). The algorithm after von Heijne (1992) predicts that these domains are of membrane spanning potential. Thus, the *Om(1E)* protein is presumed to be a transmembrane protein having two transmembrane domains flanking a short extracellular loop, provided that the translation starts from the first methionine. On the other hand, given the second methionine codon as the translation start site, the first hydrophobic domain may be a signal peptide. In this case, the *Om(1E)* protein may span the membrane at the second hydrophobic domain alone.

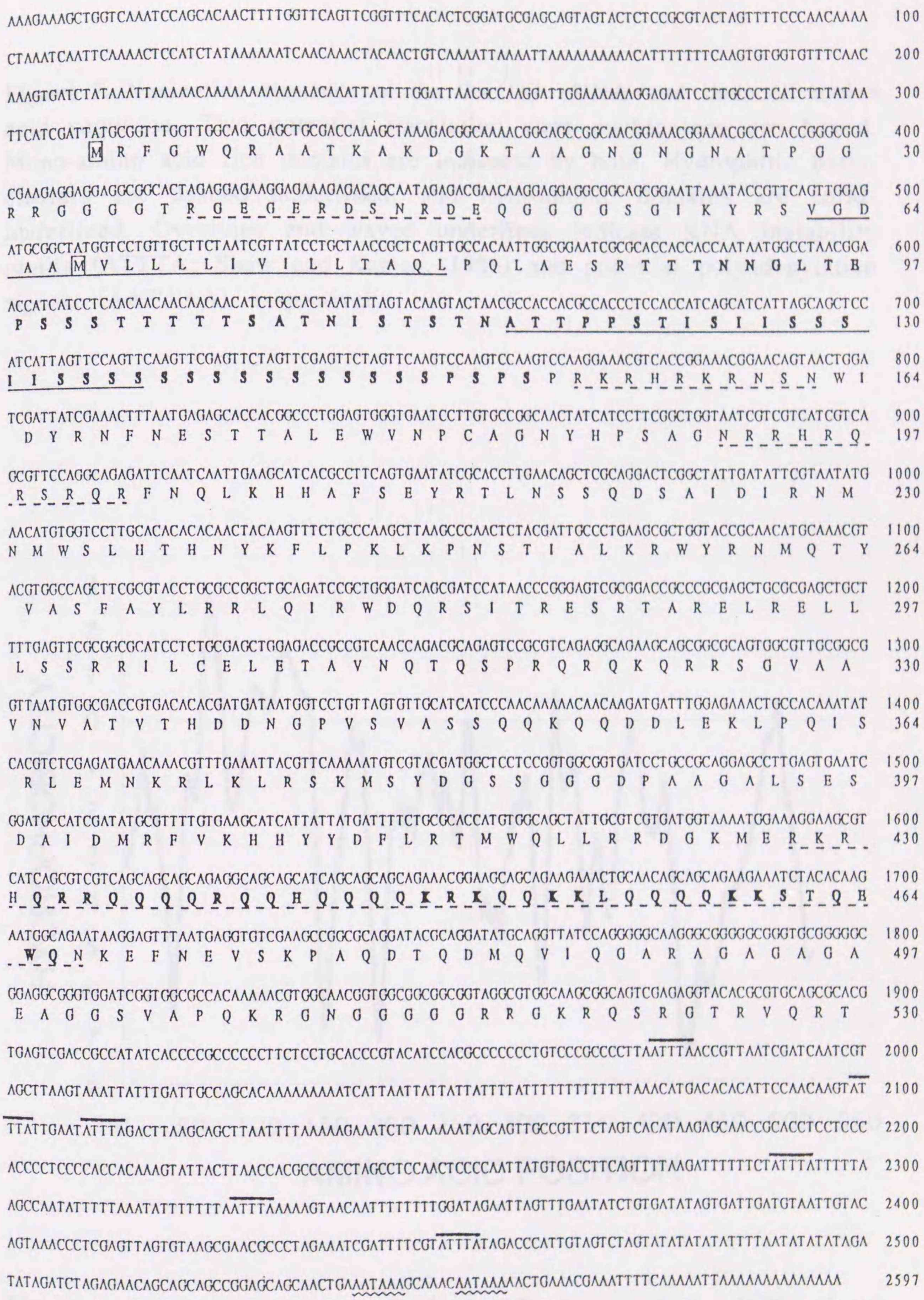

Figure 7. (*see following page for legend.*)

Figure 7. Nucleotide sequence of the *Om(1E)* cDNA and deduced amino acid sequence. Two potential translation start methionines are boxed. Mono-amino acid rich domains are indicated by bold. Hydrophilic basic-clusters are dashed underlined, and hydrophibic domains are solid-underlined. Overlines and waved underlines indicate RNA instability motifs (ATTTA; Shaw and Kamen, 1986) and potential polyadenylation signals (AATAAA), respectively.

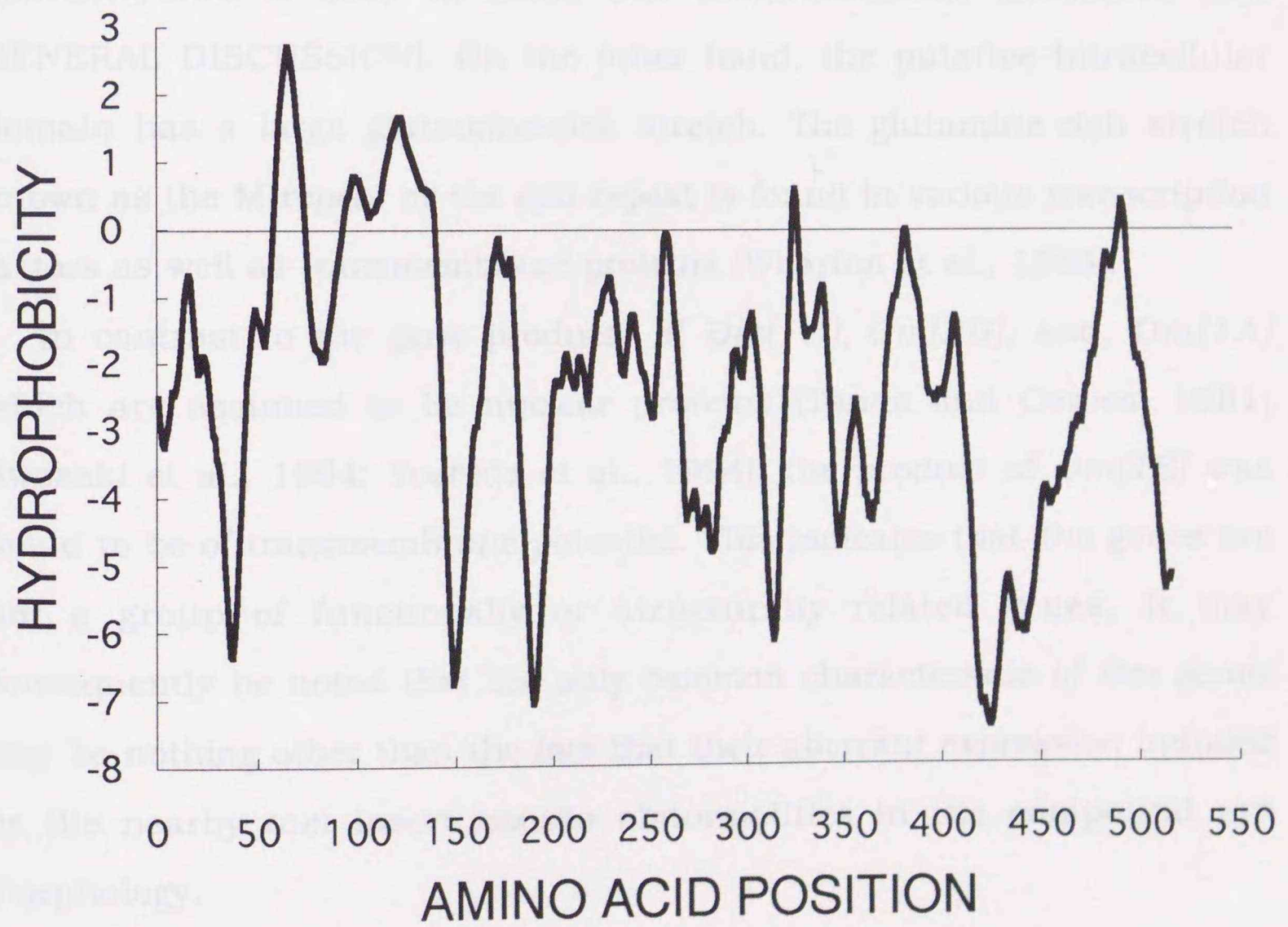

Figure 8. GES-scaled hydrophobicity plot (Engelman et al., 1986) of the putative *Om(1E)* protein.

DISCUSSION

In this study, the transcribed region t2 is shown to be the *Om(1E)* gene by three lines of evidence: first, each of the three *Om(1E)* mutants has the *tom* insertion in the vicinity of t2; second, t2 is over-expressed in the developing eye imaginal discs of all three *Om(1E)* allelic mutants; and lastly, *Drosophila melanogaster* transformants subjected to artificial t2 expression successively mimics the *Om(1E)* phenotype.

The sequence analysis have predicted that the *Om(1E)* gene encodes a novel protein having a transmembrane potential. The putative extracellular domain is highly rich in serine and threonine. Such characteristic is seen in some cell communication molecules (see GENERAL DISCUSSION). On the other hand, the putative intracellular domain has a large glutamine-rich stretch. The glutamine-rich stretch known as the M-repeat or the *opa*-repeat is found in various transcription factors as well as transmembrane proteins (Wharton et al., 1985).

In contrast to the gene products of *Om(1D)*, *Om(2D)*, and, *Om(1A)* which are assumed to be nuclear proteins (Tanda and Corces, 1991; Awasaki et al., 1994; Yoshida et al., 1994), the product of *Om(1E)* was found to be of transmembrane potential. This indicates that *Om* genes are not a group of functionally or structurally related genes. It may consequently be noted that the only common characteristic of *Om* genes may be nothing other than the fact that their aberrant expression induced by the nearby *tom* insert causes abnormalities in the compound eye morphology.

BRIEF NOTE. The nucleotide sequence data reported in this study will appear in the GSDB, DDBJ, EMBL and NCBI nucleotide sequence databases with the following accession numbers D37989 for *Om(1E)* cDNA and D37990 for t1 cDNA.

Chapter III

Spatial expression of the *Om[1E]* gene

INTRODUCTION

As a first step in inquiring into the normal function of the *Om(1E)* gene, its spatial expression was examined by *in situ* hybridization and immunocytochemistry. Because the transcript of the *Om(1E)* gene appears to be expressed during embryogenesis and imaginal development judging from Northern blot analysis (see Chapter II), I was especially interested in examining its expression in embryos and imaginal primordia of third instar larvae. In addition, phenotypic consequences of over-expression as well as repression of *Om(1E)* was examined by using transformants.

MATERIALS AND METHODS

Drosophila stocks

Drosophila ananassae stock, *ca*; *px* was used to examine the normal expression of the *Om(1E)* gene. The *Drosophila melanogaster* transformant, Hsp-*Om(1E)*, is described as Hsp-t2 in Chapter II. The Hsp-*Om(1E)*AS transformant was made as follows (see Figure 8): a 1.2-kb ClaI fragment spanning from nucleotide position 304 to 1506 of the *Om(1E)* cDNA was cloned in the BamHI site of Hsp-CaSpeR1 (see Chapter II) so as to transcribe the antisense RNA under the control of the *Hsp70* promoter. To provide the clone with a polyadenylation signal, a 0.8-kb BamHI-EcoRI fragment of *Hsp70* trailer was excised from HZ50PL (Hiromi and Gehring, 1987) and placed at the EcoRI site of Hsp-CaSpeR1. The construct was then used for *P*-element-mediated transformation as described in Chapter II. All stocks were cultured at 25

°C on standard medium containing yeast, cornmeal, malt, glucose, and agar.

Molecular and immunological techniques

Routine molecular and immunological techniques were according to Sambrook et al. (1989) .

Preparation of anti-Om(1E) antibody

A fusion protein of maltose binding protein (MBP) and part of the *Om(1E)* protein was prepared by using the Protein Fusion & Purification System (New England Bio Labs) (see Figure 1 for illustration). A HincII-SalI fragment of the *Om(1E)* cDNA corresponding to amino acids 312-530 and the termination codon (see Chapter II) was ligated to XmnI-SaI digested pMAL-c2 and introduced into *E. coli* JM109 cells. According to the manufacture's instruction, the fusion protein was over-expressed in the cells, and affinity-purified with an amylose resin column from the cell lysate. When the fusion protein was cleaved into the MBP and the *Om(1E)* protein fragment with factor Xa, the latter formed precipitates. Then, the precipitate was collected and used for immunization. The protein was emulsified with the complete Freund's adjuvant (Iratron) and injected to mice (50 μg of the protein per injection) twice at a 2-week interval. Antisera were collected two weeks later. The antibodies were affinity-purified with an antigen-bound resin column made with the *Om(1E)* protein fragment and Affi-Gel 10 (Bio-Rad) according to the manufactures

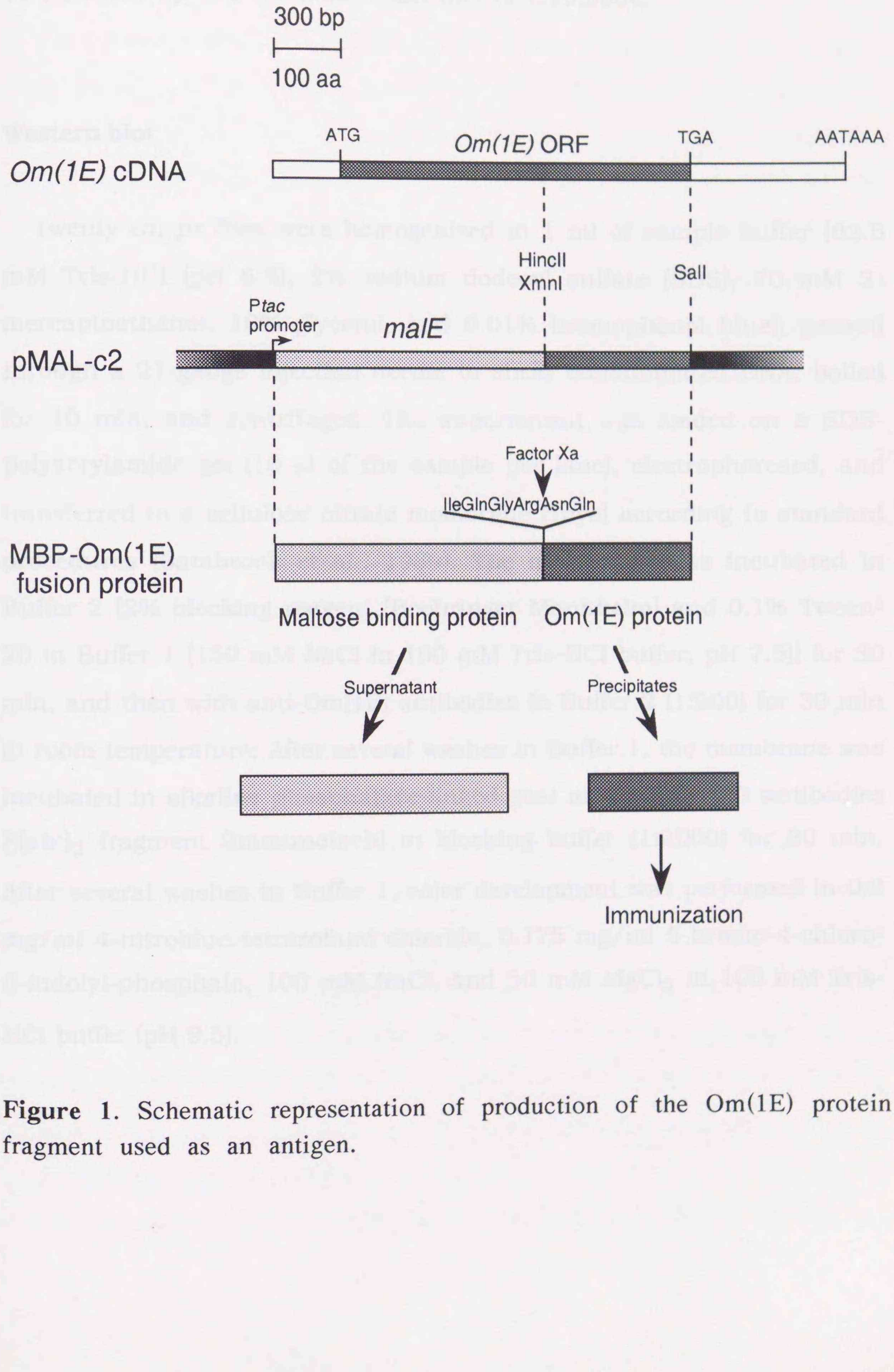

Figure 1. Schematic representation of production of the Om(1E) protein fragment used as an antigen.

instruction. The eluate of the antibody was concentrated with Centriprep-10 (Amicon) up to a minimal ELISA titer of 1:10,000<.

Western blot

Twenty *ca; px* flies were homogenized in 1 ml of sample buffer [62.5 mM Tris-HCl (pH 6.8), 2% sodium dodecyl sulfate (SDS), 70 mM 2-mercaptoethanol, 10% glycerol, and 0.01% bromophenol blue], passed through a 21-gauge injection needle to shear contaminated DNA, boiled for 10 min, and centrifuged. The supernatant was loaded on a SDS-polyacrylamide gel (10 μl of the sample per lane), electrophoresed, and transferred to a cellulose nitrate membrane (Toyo) according to standard procedures (Sambrook et al., 1989). The membrane was incubated in Buffer 2 [2% blocking reagent (Boehringer Mannheim) and 0.1% Tween-20 in Buffer 1 (150 mM NaCl in 100 mM Tris-HCl buffer, pH 7.5)] for 30 min, and then with anti-Om(1E) antibodies in Buffer 2 (1:200) for 30 min at room temperature. After several washes in Buffer 1, the membrane was incubated in alkaline phosphatase-linked goat anti-mouse IgG antibodies $F(ab')_2$ fragment (Immunotech) in blocking buffer (1:2000) for 30 min. After several washes in Buffer 1, color development was performed in 0.2 mg/ml 4-nitroblue tetrazolium chloride, 0.175 mg/ml 5-bromo-4-chloro-3-indolyl-phosphate, 100 mM NaCl, and 50 mM $MgCl_2$ in 100 mM Tris-HCl buffer (pH 9.5).

in situ hybridization to embryos and larval tissues

After Tautz and Pfeifle (1989), staged embryos were dechorionated in 50% bleach for 3 min, washed in 0.5% Triton X-100, fixed and devitellinized by vigorous shaking in equal volumes of n-heptane and 4% paraformaldehyde in HEG buffer (2 mM $MgSO_4$ and 1 mM EGTA in 100 mM HEPES, pH 6.9) for 20 min, and then in ME (50 mM EGTA in 90% methanol) briefly. The embryos were gradually rehydrated with 4% paraformaldehyde in PBS (130 mM NaCl in 10 mM phosphate buffer, pH 7.2), washed in PBT (0.1% Tween-20 in PBS), and subjected to hybridization. Preparation of larval tissues, and hybridization/detection procedures are described in Chapter II.

Immunocytochemistry

Staged embryos were dechorionated, fixed, and devitellinized as described above. Third instar larval tissues were hand-dissected and fixed in 2% paraformaldehyde in PBS for 30 min at room temperature. The embryos and the tissues were permeabilized in 0.5% Nonidet-P40 in PBS for 30 min, and then washed in PBT. The specimens were treated in PBTS (3% bovine serum albumin and 10% normal sheep serum in PBT) for 30 min, and with affinity-purified anti-Om(1E) antibody in PBTS (1:100) overnight. The specimens were then washed in PBT, and treated with horseradish peroxidase-linked sheep anti-mouse Ig antibody $F(ab')_2$ fragment (Amersham) in PBTS (1:200) for 2 hr. After several washes in PBT, the peroxidase label was visualized by incubation in 0.5 mg/ml diaminobenzidine and 0.03% H_2O_2 in PBT. The specimens were washed

in PBT, dehydrate through an ethanol series, cleared in methyl benzoate, and mounted in Bioleite (Ohken Shoji Co.).

RESULTS

Quality of anti-Om(1E) antibodies

I immunized three mice with a *Om(1E)* protein fragment expressed in *E. coli*, and obtained three lots of antibodies having a high titer against the antigen. In order to examine reactivity and specificity against Drosophila protein, three lots of antibodies were used for Western blot analyses, separately. As a result, one lot (#1) specifically recognized an approximately 55 kDa protein in fly protein extract, whereas the other lots (#2 and #3) failed to detect any protein (Figure 2). The molecular mass of 55 kDa corresponds to the predicted molecular mass of the *Om(1E)* protein, provided that it is translated from the first or the second initiation codons of the ORF (see Chapter II). Thus, the lot #1 was used for further experiments.

Expression of *Om(1E)* in developing embryos

To examine the distribution of the *Om(1E)* transcript in normal developing embryos, *in situ* hybridization experiments were performed. The *Om(1E)* transcript is not present in embryos during the early cleavage stage (Figure 3A), but first appears around nuclei locating in the apical surface of the embryo at the syncytial blastoderm stage (Figure 3B), and then accumulates in all cells at the cellular blastoderm stage

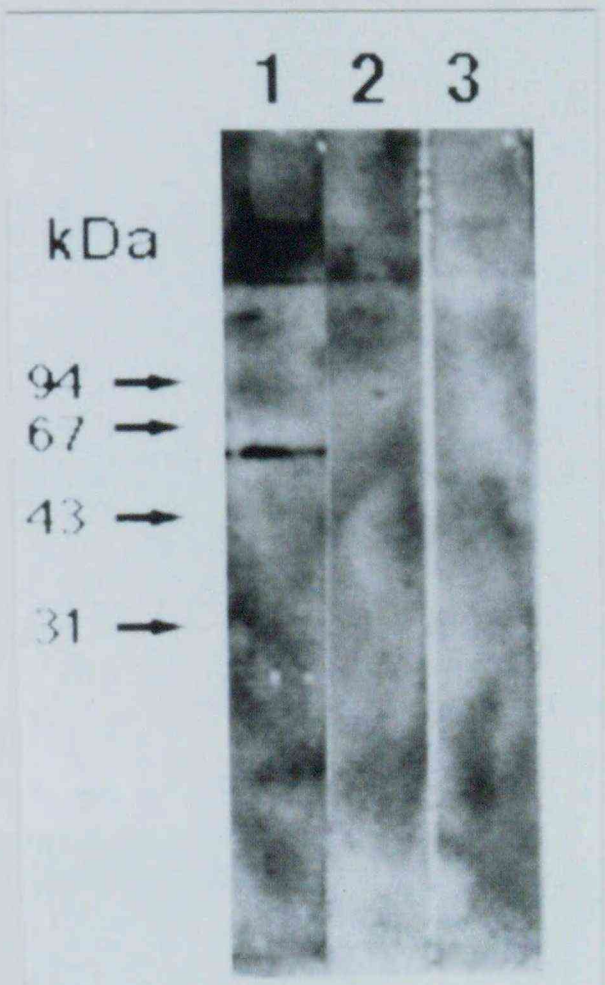

Figure 2. Western blot analysis of fly protein extract using antibodies prepared against an Om(1E) protein fragment expressed in *E. coli*. Three lots of antibodies (#1, #2, and #3) were separately used for detection.

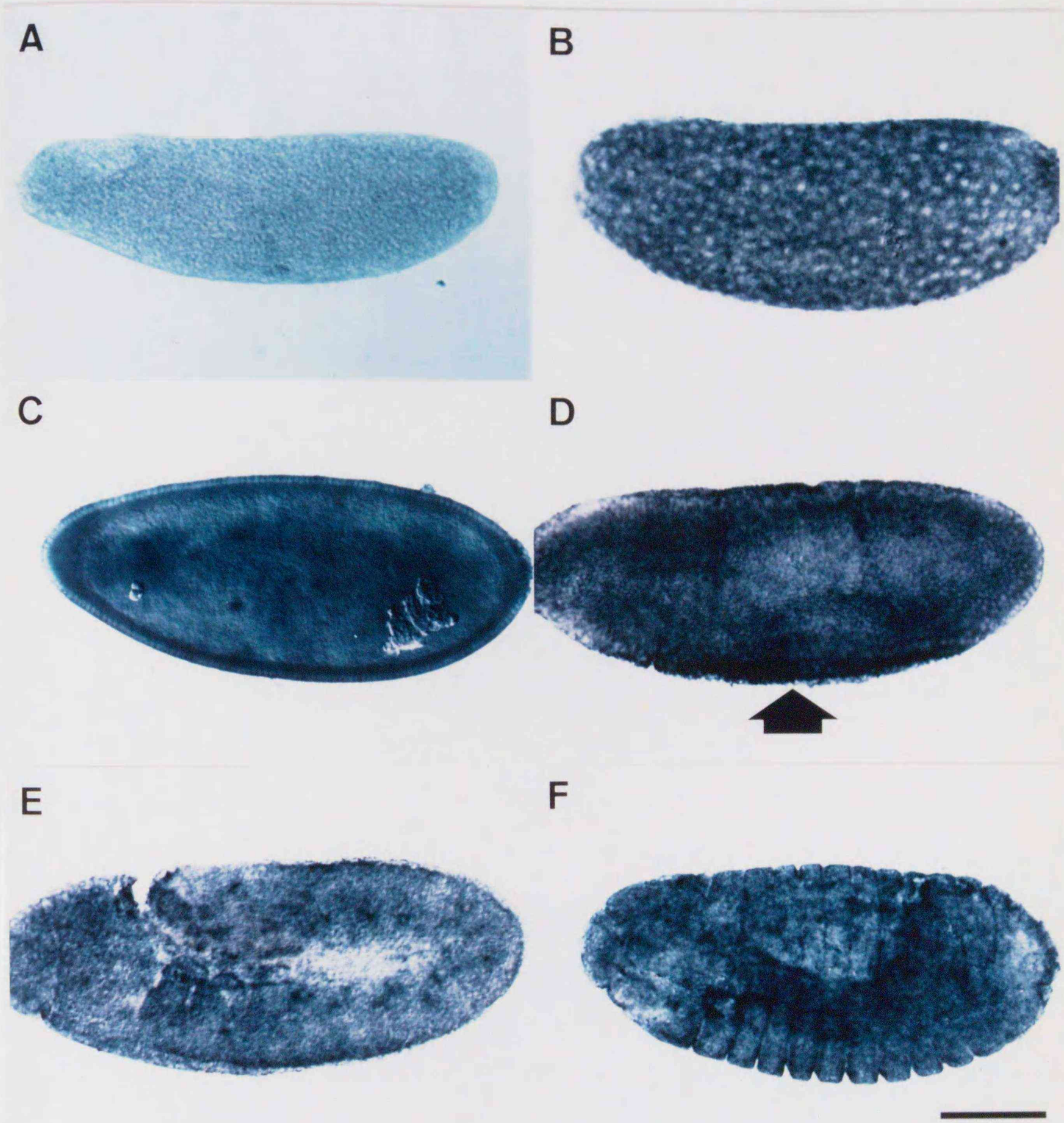

Figure 3. *in situ* hybridization to the *Om(1E)* transcript in whole mount embryos. (A) Early cleavage stage. (B) Syncytial blastoderm. The *Om(1E)* transcript is observed around nuclei (white spots). (C) Cellular blastoderm stage. (D) Ventral furrow formation stage. Note a higher level of expression in the ventral furrow (arrow). (E) Germ band extension stage. (F) Germband shortening stage. Anterior is to the left. Bar indicates 100 μm.

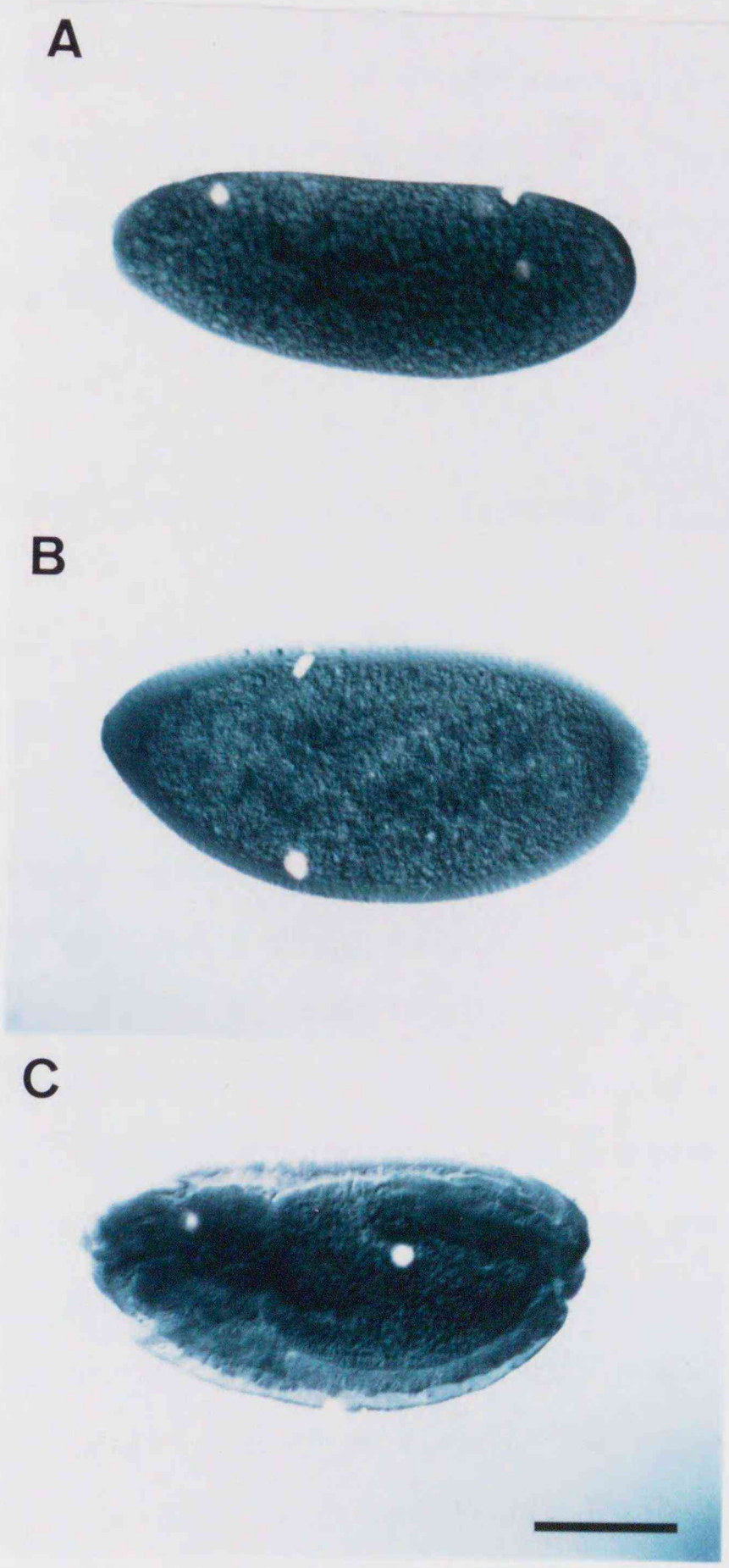

Figure 4. Immunostaining of whole mount embryos with the anti-Om(1E) antibody. (A) Syncytial blastoderm. (B) Cellular blastoderm stage. (C) Germ band shortening stage. Staining is intensified by adding 0.02% of $CoCl_2$ to the peroxidase detection reaction. Anterior is to the left. Bar indicates 100 μm.

(Figure 3C). After this stage, ubiquitous distribution of the transcript was continuously observed throughout the embryonic stage (Figures 3D-3F), although a slightly higher level of the transcript is seen in the ventral furrow during the gastrulation stage (Figure 3D). The result of the *in situ* hybridization is consistent with that of immunostaining with the anti-Om(1E) antibody (Figures 4A-4C).

Expression of *Om(1E)* in imaginal development

The expression of the *Om(1E)* gene was examined in imaginal primordia of third instar larvae. The result of *in situ* hybridization (Figures 5A-5C) and immunostaining (Figures 7A-7C) showed that the *Om(1E)* expression in imaginal discs was not restricted within any particular areas, being weak and dispersed.

On the other hand, a characteristic distribution of the *Om(1E)* transcript was observed in the central nervous system of late third instar larvae by *in situ* hybridization. While a weak expression was revealed all over the cortex of brain hemisphere and ventral ganglion, a prominent expression was seen around the entrance of the optic stalk in the brain of young third instar larvae (Figures 6A and 6B), and the region of expression later formed a distinct C-shape (Figures 6C and 6D). This region consists of an array of cells locating in the groove of the inner margin of the outer optic anlage, and matches the distribution of lamina precursor cells (for a review, see Meinertzhagen and Hanson, 1993). However, anti-Om(1E) antibody failed to stain the cortex or the lamina precursor cells, but intensely stained the neuropile (Figure 7D). This suggests that the Om(1E) protein produced in perikaryon might eventually be accumulated in the axon.

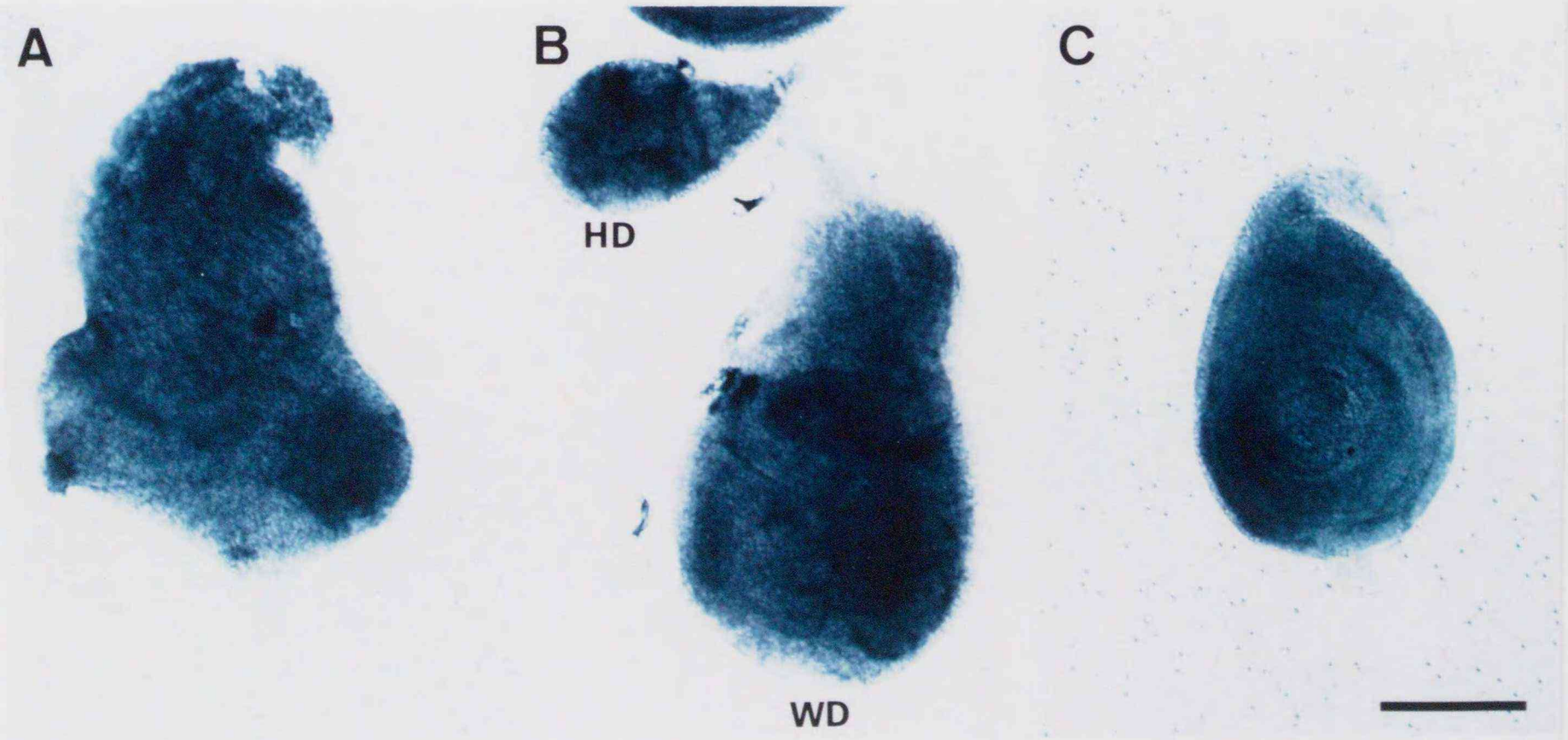

Figure 5. *in situ* hybridization to the *Om(1E)* transcript in whole mount imaginal discs of third instar larvae. (A) Eye-antenna imaginal disc. (B) Wing imaginal disc (WD) and halter imaginal disc (HD). (C) Leg imaginal disc. Bar indicates 100 μm.

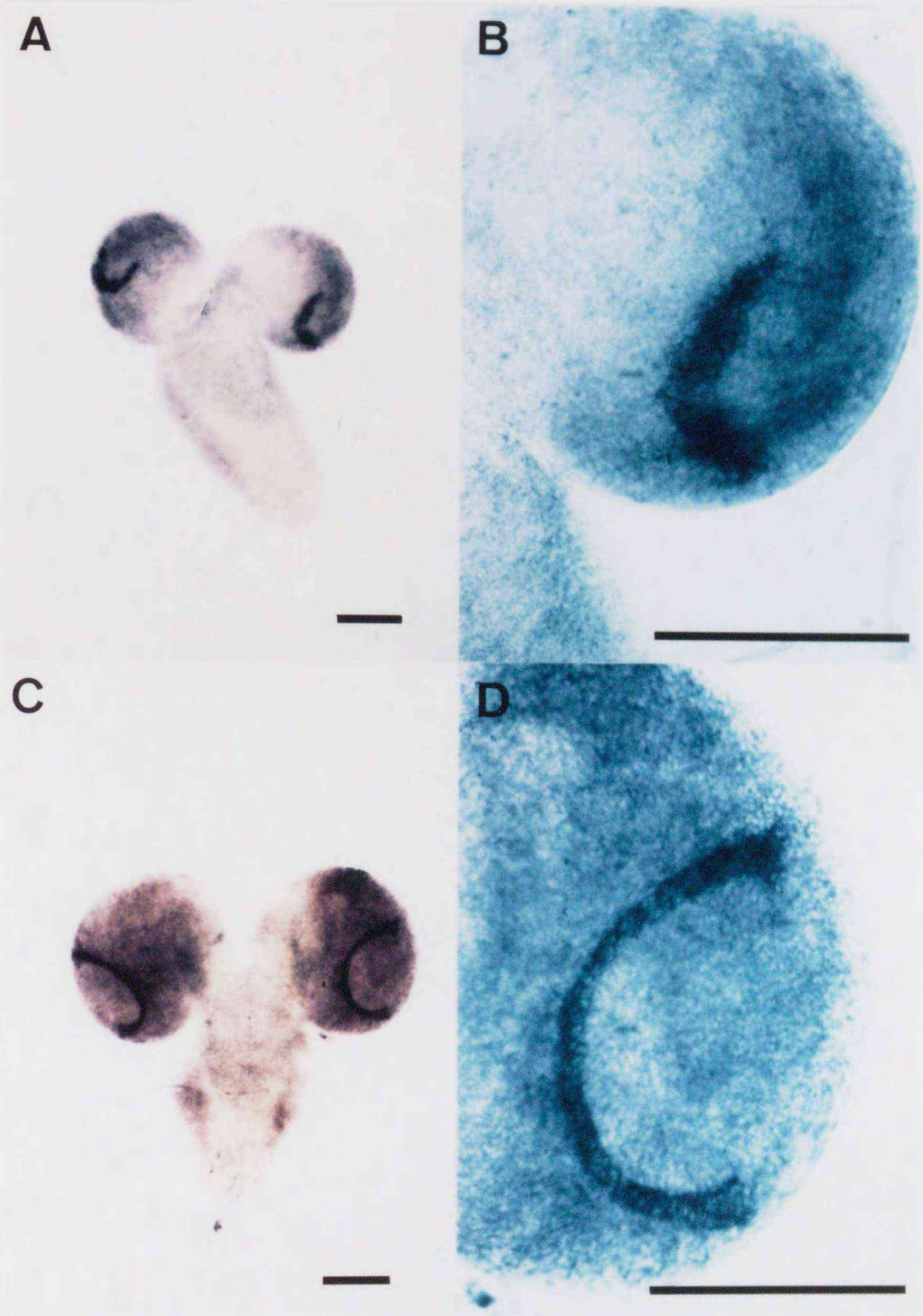

Figure 6. *in situ* hybridization to the *Om(1E)* transcript in third instar larval central nervous systems. Ventral view of whole mount preparations. Anterior is to the top. (A) Early third instar stage. (C) Late third instar stage. (B and D) Higher magnification of A and C, respectively, showing intense expression of the *Om(1E)* transcript in lamina precursor cells. Bars indicate 100 μm.

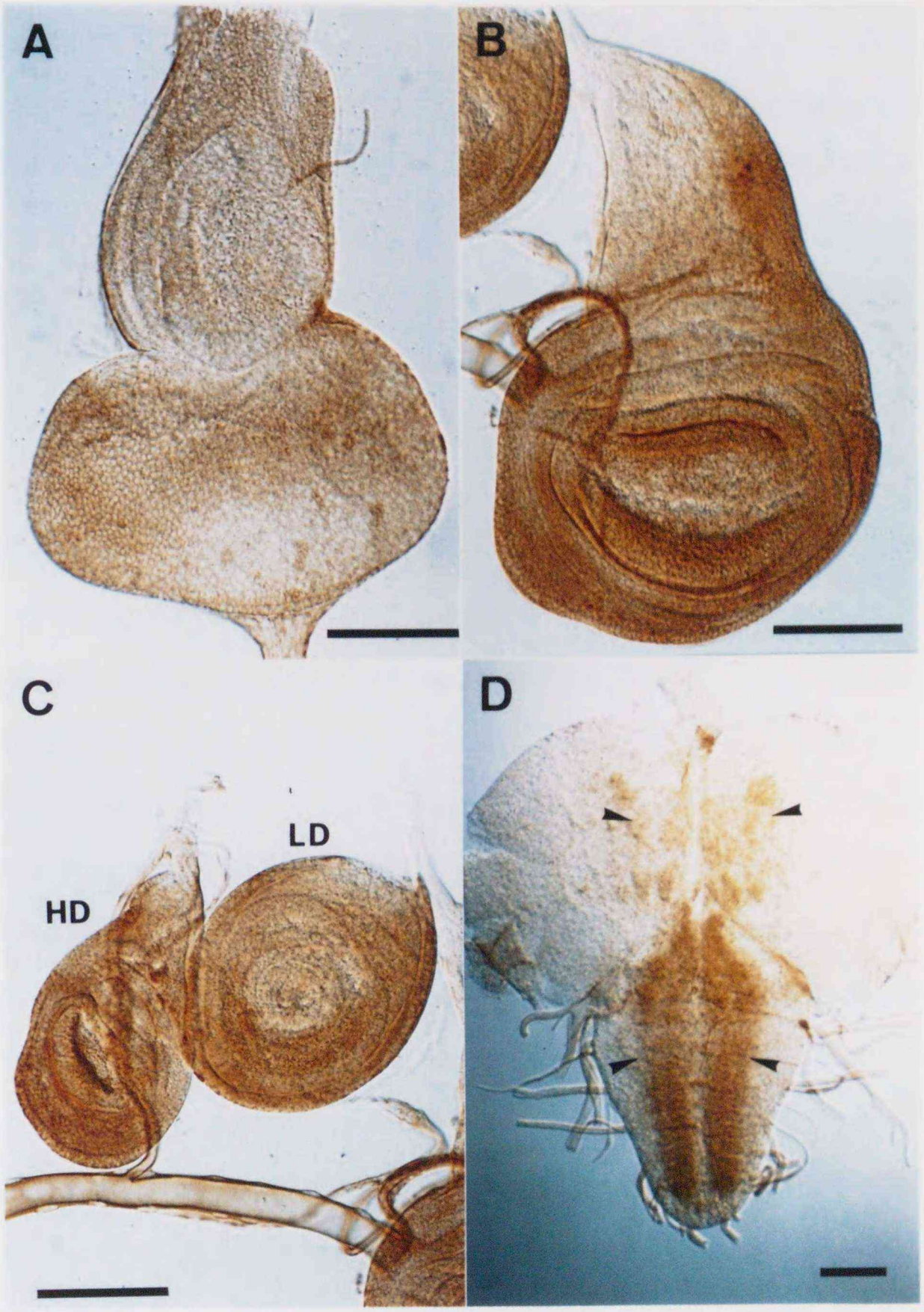

Figure 7. Immunostaining of whole mount imaginal primordia of third instar larvae with the anti-Om(1E) antibody. (A) Eye-antenna imaginal disc. (B) Wing imaginal disc. (C) Leg imaginal disc (LD) and halter imaginal disc (HD). (D) Central nervous system. Note the intense staining in the neuropile (arrow heads). Bars indicate 100 μm.

Phenotypic consequence of over-expression and suppression of *Om(1E)* in *Drosophila melanogaster* transformants

In Chapter II, I have shown that the over-expression of *Om(1E)* in developing eye imaginal discs causes overgrowth of the adult compound eye. I also examined other phenotypic effects of heat-induced ubiquitous over-expression of *Om(1E)* in embryos, third instar larvae-, and pupae using the Hsp-*Om(1E)* transformant of *Drosophila melanogaster* (Figure 8).

The Hsp-*Om(1E)* transformant appeared to be tolerant to over-expression of *Om(1E)* induced by a heat shock at 37 °C for 1 hr at any embryonic stages; most of heat-treated embryos developed to larvae and hatched without any remarkable abnormality (data not shown).

On the other hand, prominent phenotypic effects were observed in the Hsp-*Om(1E)* flies that developed from third instar larvae or early pupae which received three 1-hr heat-inductions at 37 °C at 2-hr intervals. When the transformants received the heat-induction during the early third larval instar stage, resulting flies exhibited deformation of the wing imaginal disc derivatives very often: many folds were formed around the wing hinge at the expense of the notum, the margin between the scutum and the scutellum became obscure, and the wing was held downward from the side (Figure 9B). Such phenotypes were barely observed in the Hsp-*Om(1E)* flies that had received the heat-induction during the late third larval instar to the early pupal stages. In this case, however, extra large bristles frequently appeared on the notum (Figure 9C). The extra large bristles seemed to be ectopically formed independently of native bristles, and had their own sockets (Figure 9D).

In order to examine phenotypic effects of repression of the *Om(1E)* expression, I established a *Drosophila melanogaster* transformant,

Hsp-*Om(1E)*AS (Figure 8), and induced over-expression of antisense RNA of *Om(1E)* in the transformants by heat-treatment as described above. As a result, no noticeable phenotypic effect was observed in the transformants that received heat-treatment during embryonic or larval stages (data not shown). However, when the heat-treatment was applied on early pupae of Hsp-*Om(1E)*AS, large bristles of the resulting flies often became shorter and blunter, or even disappeared leaving behind shaft-less sockets (Figures 9E and 9F).

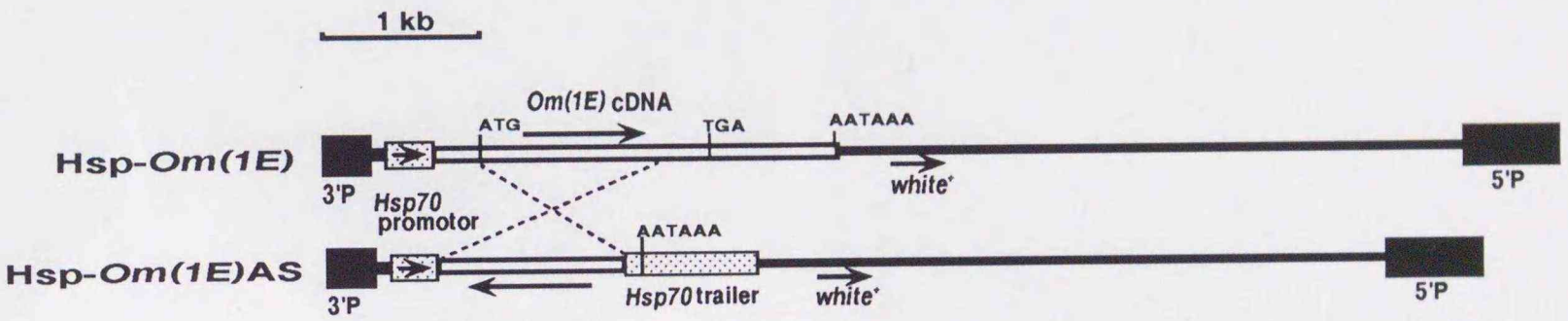

Figure 8. Schematic representation of gene constructs used for heat-induced expression of *Om(1E)* [Hsp-*Om(1E)*] and antisense RNA of *Om(1E)* [Hsp-*Om(1E)*AS].

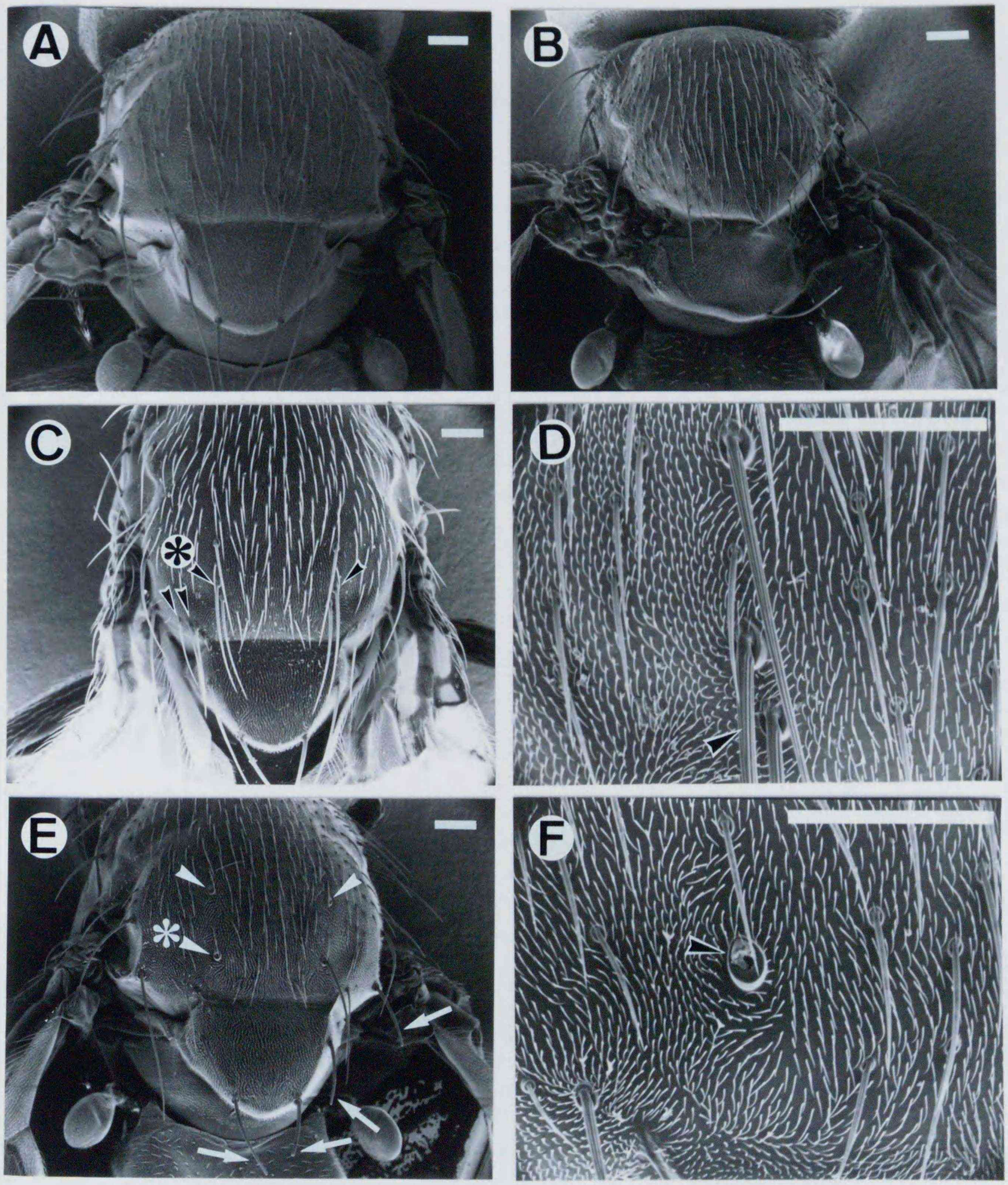

Figure 9. (*see following page for legend.*)

Figure 9. Phenotypic consequences of forced expression of *Om(1E)* or antisense RNA of *Om(1E)*. Scanning electron micrographs showing nota of transformant flies. Anterior is to the top. Bars indicate 100 μm. (A) Hsp-*Om(1E)* transformant raised under the normal condition displaying the normal phenotype. (B) Hsp-*Om(1E)* transformant received heat-induction during the early third instar larval stage. (C) Hsp-*Om(1E)* transformant received heat-induction during the late third instar larval stage. Extra large bristles are indicated by arrow heads. (D) High magnification view of the extra large bristle (arrow head) indicated by an asterisk in C. (E) Hsp-*Om(1E)*AS transformant received heat-induction during the late third instar larval stage. Large bristles often became shorter and blunter (arrows), or disappeared (arrow heads). (F) High magnification view of the bristle-missing site indicated by an asterisk in E, showing a shaft-less socket (arrow head).

DISCUSSION

in situ hybridization and immunocytochemical analyses have shown that the *Om(1E)* gene is expressed in embryos, third instar larval imaginal discs and central nervous system. Contrary to an expectation that the *Om(1E)* product, a transmembrane protein, may be found in many cells, immunostaining with anti-Om(1E) antibody failed to localize the protein in any particular class of cells and subcellular components in embryos and imaginal discs. On the other hand, the Om(1E) protein appeared to accumulate in the neuropile which consists of axons, whereas the *Om(1E)* transcript was detected in the cortex of central nervous system which consists of cell bodies. This seems to be compatible with the predicted feature of the Om(1E) protein, since various transmembrane glycoproteins such as fasciclins, neural CAMs, and connectin accumulate in axons in the nerve cord. (for a review, see Goodman and Doe, 1993).

Although the above results suggest a possible role of the *Om(1E)* gene in those tissues, this is not sufficient to understand functional aspects of the *Om(1E)* gene. One of most reliable ways to elucidate functions of a gene may be to analyze effects of mutations that completely or partially abolish the gene function of interest. Unfortunately, however, such loss-of-function mutants of the *Om(1E)* gene have not been isolated yet. In supplementation, I analyzed phenotypic effects of ubiquitous over-expression of *Om(1E)* using the Hsp-*Om(1E)* transformant. In addition, I examined effects of repression of the *Om(1E)* gene by over-expressing antisense *Om(1E)* RNA in the Hsp-*Om(1E)*AS transformant. It has been proposed to use genes producing antisense RNA (antigene) for selective inhibition of gene expression, though a perfect inhibition can not be assured in this type of experiments; antisense RNAs are considered to block its complementary mRNAs activity by forming duplexes (McGarry

and Lindquist, 1986; Bunch and Goldstein, 1989; Patel and Jacobs-Lorena, 1992). The results showed that forced over-expression of the *Om(1E)* gene during the third instar stage affects the morphogenesis of compound eye and wing imaginal disc derivatives, and that suppression of *Om(1E)* expression during early pupal stage inhibits formation of large bristles, suggesting the involvement of biological pathway affected by this gene in the development of these organ (see GENERAL DISCUSSION).

GENERAL DISCUSSION

The hypothesis put forward by Hinton (1984) that the *Om* mutations are associated with the insertion of a transposable genetic element, *tom*, has been supported by three lines of evidence that genetic locations of *Om* genes predicted from linkage studies match cytological locations of *tom* elements in *Om* mutants examined by chromosomal *in situ* hybridization (Shrimpton et al., 1986; Matsubayashi et al., 1992), that *Om(1D)* and *Om(2D)* genes have been successfully cloned by *tom*-tagging (Tanda et al., 1989; Matsubayashi et al., 1991a), and that the molecular analyses of the *Om(1D)*, *Om(2D)*, and *Om(1A)* loci have demonstrated that the *tom* elements inserted in the vicinity of the *Om* genes are responsible for mutant phenotypes (Tanda et al., 1989; Tanda and Corces, 1991; Matsubayashi et al., 1991a; 1991b; Awasaki et al., 1994; Yoshida et al., 1994). The present study shows that this holds true for another *Om* mutation, *Om(1E)*, which exhibits their own peculiar phenotypes that compound eyes are enlarged dorso-posteriorly without marked disorganization of ommatidial structures, in contrast to all the other *Om* mutations characterized by deformed compound eyes having fewer-than-normal ommatidia.

The *Om(1E)* mutation is similar to the other *Om* mutations in that the *tom* element inserted in the vicinity of the *Om* gene enhances the gene expression. In the *Om(1A)*, *Om(1D)*, and *Om(2D)* mutations, the *tom* inserts responsible for the mutant phenotypes reside in the regions up to 70 kb downstream of transcription initiation sites, and their directions are either parallel or reverse to those of *Om* genes. In this respect, *Om(1E)59a* and *Om(1E)109* are similar to those *Om* mutants, but

Om(1E)53 differs from the others in that the *tom* insert resides 15 kb upstream of the transcription initiation site of the *Om(1E)* gene.

The *Om(1E)53* mutant also differs from the others in that the *tom* insert exerts a positive effect on expression of another nearby gene, t1, although over-expression of the gene appears to be limited only in eye imaginal discs, and does not result in any abnormal phenotype. This is in contrast to the case of *Om(2D)* mutants; the *tom* insert responsible for the mutant phenotype has no detectable effects on the ornithine aminotransferase (OAT) precursor gene present near the insertion site, but affect the *Om(2D)* gene located farther distally (Yoshida et al., 1994).

It is an interesting question why *tom* elements cause *Om* mutations. Almost all mutations so far obtained in the *Om* mutability system causes defects in the morphology of adult compound eye, although the *tom* element is found in a number of loci in the genome. This means that *tom* may have no preference of insertion sites, but it mutates *Om* genes when it is fortuitously inserted in their neighborhood.

In an early phase of studies on *Om* mutations, it was assumed that the *Om* genes involved in eye morphogenesis, so that the *Om* mutability system would be useful for molecular analyses of eye morphogenesis. Unfortunately, however, this was not the case; the *Om(1A)* gene happens to be *cut*, and the *Om(2D)* gene does not seem to be expressed so much as to be detected by *in situ* hybridization of wild-type eye imaginal discs. Taking into account all the findings so far obtained by molecular analyses of *Om* mutants, a most plausible explanation as to why the *tom* element induces *Om* mutations may be that the *tom* element carries an enhancer sequence or sequences which act on nearby genes with the help of an eye-disc specific regulatory factor, and that the *Om* genes might be a set of genes, the products of which exert influence upon eye morphogenesis when present in excess.

Similar to *Om* mutations are some retrotransposon- or retrovirus-induced gain-of-function mutations. In *Drosophila melanogaster*, insertions of the *gypsy* and *copia* elements give rise to a few gain-of-function mutations of the *achaete-scute* complex, e. g. *Hairy-wing*^{1} (*Hw*^{1}): in *Hw*^{1}, the *gypsy* element inserts in the *achaete* gene resulting in truncation and over-production of the transcript (Campuzano et al., 1986). The *Hw*^{1} mutation is suppressible by a loss-of-function mutation, *suppressor-of-Hairy-wing* [*su(Hw)*], suggesting that the over-expression in *Hw*^{1} is driven by the *su(Hw)* protein bound within the 5' untranslated region of the *gypsy* element (Mazo et al., 1989). In the case of yeast ROAM mutations, over-expression of various genes are induced by the *MAT* locus-dependent enhancer present in the 5' leader sequence of Ty1 insertions (for a review, see Boeke, 1989). Ty1 elements in ROAM mutations locate exclusively in the juxtaposition of target gene promoters in the opposite direction. Most analogous with the *Om* mutations are tumorigenetic mutations in vertebrates which are induced by retroviral proviruses (for a review, see Nusse, 1986). For example, the provirus of mouse mammary tumor virus (MMTV) activates the expression of several heterologous proto-oncogenes including *int-1* (*Wnt-1*) and *int-2* when inserted into loci either upstream or downstream of the target gene promoters, sometimes more than 10 kb apart (for a review, see Nusse, 1988). The *int* genes are not expressed in normal mammary glands, but their expression is stimulated when the provirus inserts in their vicinity specifically in the organ under the influence of steroid hormones. In this case, over-expression of the gene is brought about by a cooperative action of the hormone response element (Chandler et al., 1983; Scheidereit et al., 1983) and the mammary gland specific enhancer (Lefebvre et al., 1991; Mink et al., 1992; Mok et al., 1992) carried by the MMTV LTR.

Recently, Mozer and Benzer (1994) have reported that the *17.6* transposable element of *Drosophila melanogaster*, which has a considerable homology with the *tom* element (Tanda et al., 1988) and the avian leukosis-sarcoma viral genome (Kugimiya et al., 1983), possesses lamina precursor cell-specific and eye imaginal disc-specific enhancers within its LTR. Thus, it is not rare that retrotransposons have tissue specific enhancers in their LTRs which can act positively on relevant genes. To demonstrate the presence of tissue-specific enhancer in the *tom* LTR, I have ligated a *tom* LTR with *lacZ* and transformed *Drosophila melanogaster* with this construct. As a result, it was found that the *tom* LTR is indeed effective in inducing *lacZ* expression in eye imaginal discs (unpublished data). Taking advantage of this, I have made constructs containing a *tom* LTR and cDNA sequences, and tested in the present study if transformants carrying these constructs mimic the *Om(1E)* phenotype. The results have clearly indicated that the *tom* LTR indeed possesses an eye imaginal disc-specific enhancer.

Involvement of a tissue specific enhancer of the *tom* element in over-expression of adjacent genes alone can not explain why some genes such as *Om* genes are affected by the *tom* insert, but others such as the OAT precursor gene is not. Position of *tom* inserts may be an important factor, since t1 expression seems to be affected by the *tom* insert residing 5 kb upstream in *Om(1E)53*, but not by the *tom* insert 20 kb downstream in *Om(1E)59a* or *Om(1E)109*. However, the proximity of *tom* insert to target gene is not a determinative factor in the *tom*-driven over-expression; the *tom* inserts in *Om(2D)* mutants do not affect the most proximal gene, i. e., the OAT precursor gene. Thus, it is assumed that the enhancer in the *tom* element might selectively interact with a given type of transcriptional elements. For instance, defective P elements can activate the glucose-6-phosphate dehydrogenase (G6PD) promoter but

not the normal actin 5C promoter. However, the actin 5C promoter can be activated by the *P* element if the 20 bp sequence around the G6PD transcription start site is present in front of the promoter (Ito et al., 1993). It has also been reported that when the synthetic polymerase II promoter is linked to a reporter gene with different combinations of upstream promoter elements and enhancer elements, the activity of the promoter varies depending on the combination of the elements (Wang and Gralla, 1991). In order to examine if *Om* genes share such a common regulatory sequence, Yoshida et al. (1994) have compared upstream regions of the *Om(1D)* and *Om(2D)* genes, and found that 28-bp sequences located 207 bp and 99 bp upstream of the transcriptional start sites, respectively, are 78.6 % homologous to each other. However, a preliminary Southern blot analysis with the *Om(1E)* gene failed to locate a similar sequence in its upstream region. Furthermore, the transformation studies have suggested that the presumptive *tom* enhancer stimulates a heterologous promoter such as the *Hsp70* promoter. Thus, the discriminative factor responsible for the differential action of *tom* on adjacent gene expression remains unclear.

The adult compound eye of *Om(1E)* mutants looks like as if one extra eye is fused dorso-posterially on another. The extra eye appears to be originated from a bud protruding from the eye imaginal disc at the third larval instar stage. The arrangement of ommatidia is basically normal except that the polarity is disturbed in some ommatidia around the mirror image symmetry line which appears to be at the boundary of two overlapping eyes. Thus, pattern formation appears to be taken place in *Om(1E)* mutants regarding the extra portion of eye as part of a single eye. In this respect, the *Om(1E)* phenotype differs from the *extra-eye* (Marcey and Stark, 1985) and *two-faced* (Lipshitz and Kankel, 1985) phenotypes

of *Drosophila melanogaster* where an extra compound eye is formed independently of another. Furthermore, the *Om(1E)* mutation differs from the $Notch^{ts1}$ mutation (Cagan and Ready, 1989) or the *scabrous* mutation (Baker et al., 1990) of *Drosophila melanogaster* which results in recruitment of cells of different fates for excess photoreceptor precursor cells, since the *Om(1E)* phenotype appears to be caused by increasing the number of undifferentiated cells in the eye imaginal disc.

The presumptive *Om(1E)* gene product is a novel transmembrane protein containing stretches of mono-amino acids such as glutamine, serine, and threonine. The glutamine-rich stretch is seen in various transcription factors as well as transmembrane proteins such as Notch (Wharton et al., 1985). The *Om(1E)* protein is likely to have either one or two membrane spanning domains. In either case, the putative extracellular domain is highly rich in serine and threonine (about 50 %). Serine/threonine-rich extracellular domains are seen in several proteins which appear to be involved in cell interaction, such as a-agglutinin attachment subunit of yeast (Roy et al., 1991), cell surface antigen 114/A10 of mouse (Doughery et al., 1989), and zipper protein of Drosophila (Zhao et al., 1988), and are considered to be subject to O-glycosylation. Thus, the possibility may be envisaged that the *Om(1E)* gene product is a glycoprotein involving in intercellular communication which may be required for the growth control of imaginal discs. This idea is consistent with the knowledge that contact-dependent cell interactions may play an important role in regulating growth of imaginal discs. It has been known that overgrowth of imaginal disc epithelia resulted from loss-of-function of tumor suppressor genes often have defects in cell communication (Ryerse and Nagel, 1984; Jursnich et al., 1990; for a review, see Cohen, 1993). However, the function of the

Om(1E) gene seems to be contrary to that of tumor suppressor genes; tumor suppressor genes are required to stop cell proliferation, whereas the *Om(1E)* product may promote cell proliferation, because its excess expression leads to overgrowth of the compound eye.

Whole mount *in situ* hybridization and immunocytochemical studies have shown ubiquitous expression of the *Om(1E)* gene in embryonic cells, developing imaginal discs, and larval central nervous system in normal individuals. Although these results suggest a possible role of the *Om(1E)* gene in those tissues, its actual function remains to be explored. Nevertheless, forced over-expression of the *Om(1E)* gene during the early third instar stage affects the morphogenesis of compound eye and notum in the transformants, suggesting the existence of a biological pathway affected by this gene in the development of these organs. In addition, extra large bristles are induced by over-expression of the *Om(1E)* gene during the late larval or the early pupal stage. This phenotype mimics that caused by mutations of genes involved in differentiation of the sensory organ precursor cell, such as gain-of-function mutations of the *achaete* and/or *scute* genes, or loss-of-function mutations of neurogenic genes (for reviews, see Ghysen and Dambly-Chaudriere, 1989; Simpson, 1990; Campuzano and Modolell, 1992). Conversely, suppression of the *Om(1E)* expression by the antisense RNA during an early pupal stage interferes with the large bristle formation resulting in short bristle or shaft-less socket phenotypes. The shaft-less socket phenotype is seen in loss-of-function mutations of the *Hairless* gene which is required for bristle differentiation from daughter cells of sensory organ precursor cells (Bang and Posakony, 1992). Interestingly, *Hsp70* promoter-driven over-expression of *Hairless* in a transformant also causes extra bristle formation, as in the case of neurogenic mutations or

over-expression of *Om(1E)*. Taken together, the *Om(1E)* gene is assumed to play a role in differentiation of the external sensory organ.

On the other hand, the *Om(1E)* gene is prominently expressed in lamina precursor cells. The intense *Om(1E)* expression is limited in lamina precursor cells which are present in the groove of the inner margin of outer optic anlage, but not in the lamina cortex. This suggests a possible *Om(1E)* function in an early phase of lamina cell differentiation. This is particularly of interest, because the lamina is currently one of the most interesting topics in Drosophila biology. A great number of morphological, developmental, and physiological studies on the lamina have been accumulated, and the lamina is the best characterized nervous system in Drosophila at present (for a review, see Meinertzhagen and Hanson, 1993). The lamina precursors differentiate to the lamina cortex through a wave of mitosis at the groove in response to progressive innervation of photoreceptor axons, implying cell-interaction dependent differentiation (Hofbauer and Campos-Ortega, 1990; Selleck et al., 1992). This seems to be consistent with the above notion that the *Om(1E)* protein might be involved in cell interaction and cell proliferation. Recently, surveys of genes controlling development of the imaginal central nervous components including the lamina are in progress (Kretzschmar et al., 1991; Tix et al., 1991; Datta et al., 1993; Selleck et al., 1994). However, only a few genes have been characterized in this field of researches, and little is known about the genetic basis of the lamina development. Thus, the *Om(1E)* gene might provide a breakthrough for this query. This merits further elaboration.

REFERENCES

Awasaki, T., Juni, N., Hamabata, T., Yoshida, K., Matsuda, M., Tobari, Y. N., and Hori, S. H. (1994). Retrotransposon-induced ectopic expression of *cut* causes the *Om(1A)* mutant in *Drosophila ananassae*. Genetics 137, 165-174.

Baker, N. E., Mlodzik, M., and Rubin, G. M. (1990). Spacing differentiation in the Developing *Drosophila* eye: a fibrinogen-related lateral inhibitor encoded by *scabrous*. Science 250, 1370-1377.

Bang, A. G., and Posakony, W. (1992). The *Drosophila* gene *Hairless* encodes a novel basic protein that controls alternative cell fates in adult sensory organ development. Genes Dev. 6, 1752-1769.

Bender, W., Spierer. P., and Hogness, D. S. (1983). Chromosomal walking and jumping to isolate DNA from the *Ace* and *rosy* loci and the Bithorax complex in *Drosophila melanogaster*. J. Mol. Biol. 168, 17-33.

Bingham, P. M., Kidwell, M. G., and Rubin, G. M. (1982). The molecular basis of P-M hybrid dysgenesis: the role of the P element, a P-strain-specific transposon family. Cell 29, 995-1004.

Bishop, J. G., III, and Corces, V. G. (1988). Expression of an activated *ras* gene causes developmental abnormalities in transgenic *Drosophila melanogaster*. Genes Dev. 5, 567-577.

Blochlinger, K., Bodmer, R., Jack, J., Jan, L. Y., and Jan, Y. N. (1988). Primary structure and expression of a product from *cut*, a locus involved in specifying sensory organ identity in *Drosophila*. Nature 333, 629-635.

Blochlinger, K., Jan, L. Y., and Jan, Y. N. (1991). Transformation of sensory organ identity by ectopic expression of Cut in *Drosophila*. Genes Dev. 5, 1124-1135.

Bodmer, R., Barbel, S., Sheperd, S., Jack, J. W., Jan, L. Y., and Jan, Y. N. (1987). Transformation of sensory organs by mutation of the *cut* locus of D. melanogaster. Cell 51, 293-307.

Boeke, J. D. (1989). Transposable elements in *Saccharomyces cerevisiae*. In Mobile DNA, D. E. Berg and M. M. Howe, eds., (Washington D. C.: American Society for Microbiology), pp 335-374.

Bradley, D., Carpenter, R., Sommer, H., Hartley, N., and Coen, E. (1993). Complementary floral homeotic phenotypes result from opposite orientations of a transposon at the *plena* locus of Antirrhinum. Cell 72, 85-95.

Bunch, T. A., and Goldstein, L. S. (1989). The conditional inhibition of gene expression in cultured Drosophila cells by antisense RNA. Nucl. Acids Res. 17, 9761-9782.

Cagan, R. L., and Ready, D. F. (1989). *Notch* is required for successive cell decisions in the developing *Drosophila* retina. Genes Dev. 3, 1099-1112.

Campuzano, S., and Modolell, J. (1992). Patterning of the *Drosophila* nervous system: the *achaete-scute* gene complex. Trends Genet. 8, 202-208.

Campuzano, S., Balcells, L., Villares, R., Carramolino, L., García-Alonso, L., and Modolell, J. (1986). Excess function *Hairy-wing* mutations caused by *gypsy* and *copia* insertions within structural genes of the *achaete-scute* locus of Drosophila. Cell 44, 303-312.

Cavener, D. R. (1987). Comparison of the consensus sequence flanking translational start sites in *Drosophila* and vertebrates. Nucl. Acids Res. 1987, 1353-1361.

Chandler, V. L., Maler, B. A., and Yamamoto, K. R. (1983). DNA sequences bound specifically by glucocorticoid receptor in vitro render a heterologous promoter hormone responsive in vivo. Cell 33, 489-499.

Cohen, S. M. (1993). Imaginal disc development. In The development of Drosophila melanogaster, M. Bate and A. M. Arias, eds., (Plainview, New Yolk: Cold spring Harbor Laboratory Press), pp 747-841.

Cox, K. H., Deleon, V. D., Angerer, L. M., and Angerer, R. C. (1984). Detection of mRNAs in sea urchin embryos by *in situ* hybridization using asymmetric RNA probes. Dev. Biol. 101, 485-502.

Datta, S., Stark, K., and Kankel, D. R. (1993). Enhancer detector analysis of the extent of genomic involvement in nervous system development in *Drosophila melanogaster*. J. Neurobiol. 24, 824-841.

Dickson, B., and Hafen, E. (1993). Genetic dissection of eye development in *Drosophila*. In The development of Drosophila melanogaster, M. Bate and A. M. Arias, eds., (Plainview, New Yolk: Cold spring Harbor Laboratory Press), pp 1327-1362.

Doughery, G. J., Kay, R. J., and Humphries, R. K. (1989). Molecular cloning of 114/A10, a cell surface antigen containing highly conserved repeated elements, which is expressed by murine hemopoietic progenitor cells and interleukin-3-dependent cell lines. J. Biol. Chem. 264, 6509-6514.

Engelman, D. M., Steitz, T. A., and Goldman, A. (1986). Identifying nonpolar transbilayer helices in amino acid sequences of membrane proteins. Annu. Rev. Biophys. Biophys. Chem. 15, 321-353.

Engels, W. R., Preston, C. R., Thompson, P., and Eggleston, W. B. (1986). *In situ* hybridization to Drosophila salivary chromosomes with biotinylated DNA probes and alkaline phosphatase. Focus 8, 6-8.

Georgiev, G. P. (1984). Mobile genetic elements in animal cells and their biological significance. Eur. J. Biochem. 145, 203-220.

Ghysen, A., and Dambly-Chaudriere, C. (1989). Genesis of the *Drosophila* peripheral nervous system. Trends Genet. 5, 251-255.

Goodman, C. S., and Doe, C. Q. (1993). Embryonic development of the *Drosophila* central nervous system. In The development of Drosophila melanogaster, M. Bate and A. M. Arias, eds., (Plainview, New Yolk: Cold spring Harbor Laboratory Press), pp 1131-1206.

Hake, S. (1992). Unraveling the knots in plant development. Trends Genet. 8, 109-114.

Henikoff, S. (1984). Unidirectional digestion with exonucleaseIII creates targeted breakpoints for DNA sequencing. Gene 28, 351-359.

Higashijima, S., Kojima, T., Michiue, T., Ishimaru, S., Emori, Y., and Saigo, K. (1992a). Dual *Bar* homeo box genes of *Drosophila* required in two photoreceptor cells, R1 and R6, and primary pigment cells for normal eye development. Genes Dev. 6, 50-60.

Higashijima, S., Michiue, T., Emori, Y., and Saigo, K. (1992b). Subtype determination of *Drosophila* embryonic external sensory organs by redundant homeo box genes *BarH1* and *BarH2*. Genes Dev. 6, 1005-1018.

Hinton, C. W. (1984). Morphogenetically specific mutability in *Drosophila ananassae*. Genetics 106, 631-653.

Hiromi, Y., and Gehring, W. J. (1987). Regulation and function of the Drosophila segmentation gene *fushi tarazu*. Cell 50, 963-974.

Hofbauer, A., and Campos-Ortega, J. A. (1990). Proliferation pattern and early differentiation of the optic lobes in *Drosophila melanogaster*. Roux's Arch. Dev. Biol. 198, 264-274.

Ito, H., Yoshida, K., and Hori, S. H. (1989). Positive regulation of the *Drosophila melanogaster* G6PD gene by an insertion sequence. Biochem. Genet. 27, 379-393.

Ito, H., Hamabata, T., and Hori, S. H. (1993). Transcriptional activation of the Drosophila melanogaster glucose-6-phosphate dehydrogenase gene by insertion of defective P elements. Mol. Gen. Genet. 241, 637-646.

Itoh, M., Iwabuchi, M., Yorimoto, N., and Hori, S. H. (1988). A transposable genetic element associated with positive regulation of G6PD gene expression in *Drosophila melanogaster*. Genet. Res. 52, 169-177.

Janknecht, R., Sanger, C., and Pongs, O. (1991). $(HX)_n$ repeats: a pH-controlled protein-protein interaction motif of eukaryotic transcription factors? FEBS Lett. 295, 1-2.

Jowett, T. (1986). Preparation of nucleic acids. In Drosophila: a practical approach, D. B. Roberts, eds., (Oxford, Washington DC: IRL PRESS), pp 275-286.

Jursnich, V. A., Fraser, S. E., Held, L. I., Jr., Ryerse, J., and Bryant, P. J. (1990). Defective gap-junctional communication associated with imaginal disc overgrowth and degeneration caused by mutations of the *dco* gene in *Drosophila*. Dev. Biol. 140, 413-429.

Karess, R. E., and Rubin, G. M. (1984). Analysis of P transposable element function in Drosophila. Cell 38, 135-146.

Kojima, T., Ishimaru, S., Higashijima, S., Takayama, E., Akimaru, H., Sone, M., Emori, Y., and Saigo, K. (1991). Identification of a different-type homeobox gene, *BarH1*, possibly causing Bar (*B*) and *Om(1D)* mutation in *Drosophila*. Proc. Natl. Acad. Sci. USA 88, 4343-4347.

Kretzschmar, D., Pflugfelder, G., Schneuwly, S., and Heisenberg, M. (1991). Enhancer-trap cloning on two genes expressed in the lamina of Drosophila melanogaster. J. Neurogenet. 7, 131. (Abstact).

Kugimiya, W., Ikenaga, H., and Saigo, K. (1983). Close relationship between the long terminal repeats of avian leukosis-sarcoma virus and *copia*-like movable genetic elements of *Drosophila*. Proc. Natl. Sci. USA 80, 3193-3197.

Kushida, H., Kushida, T., and Iijima, H. (1985). An improved method for both light and electron microscopy of identical sites in semi-thin sections under 200 kV transmission electron microscope. J. Electron Microsc. 34, 411-438.

Lefebvre, P., Berard, D. S., Cordingley, M. G., and Hager, G. L. (1991). Two Regions of the mouse mammary tumor virus long terminal repeat regulate the activity of its promoter in mammary cell lines. Mol. Cell. Biol. 11, 2529-2537.

Lindsley, D. L., and Zimm, G. G. (1992). The genome of *Drosophila melanogaster* (San Diego, California: Academic Press).

Lipshitz, H. D., and Kankel, D. R. (1985). Developmental interactions between the peripheral and central nervous system in *Drosophila melanogaster*: analysis of the mutant, *two-faced*. Dev. Biol. 107, 1-12.

Marcey, D. J., and Stark, W. S. (1985). The morphology, physiology, and neural projections of supernumerary compound eyes in *Drosophila melanogaster*. Dev. Biol. 107, 180-197.

Matsubayashi, H., Juni, N., Usui, K., Hori, S. H., and Tobari, Y. N. (1991a). Molecular and histological characterizations of the *Om(2D)* mutants in *Drosophila ananassae*. Mol. Gen. Genet. 227, 165-172.

Matsubayashi, H., Tobari, N. T., and Hori, S. H. (1991b). Genetic analysis of the *Om(2D)* locus in *Drosophila ananassae*. Jpn. J. Genet. 66, 387-397.

Matsubayashi, H., Matsuda, M., Tomimura, Y., Shibata, M., and Tobari, Y. N. (1992). Cytological mapping of *Om* mutants of *Drosophila ananassae*. Jpn. J. Genet. 67, 259-264.

Mazo, A. M., Mizrokhi, L. J., Karavanov, A. A., Sedkov, Y. A., Krichevskaja, A. A., and Ilyin, Y. V. (1989). Suppression in *Drosophila*: *su(Hw)* and *su(f)* gene products interact with a region of *gypsy* (*mdg4*) regulating its transcriptional activity. EMBO J. 8, 903-911.

McGarry, T. J., and Lindquist, S. (1986). Inhibition of heat shock protein synthesis by heat-inducible antisense RNA. Proc. Natl. Acad. Sci. USA 83, 399-403.

Meinertzhagen, I. A., and Hanson, T. E. (1993). The development of the optic lobe. In The Development of Drosophila melanogaster, M. Bate and A. M. Arias, eds., (Plainview, New York: Cold Spring Harbor Laboratory Press), pp 1363-1491.

Mink, S., Härtig, E., Jennewein, P., Doppler, W., and Cato, A. C. B. (1992). A mammary cell-specific enhancer in mouse mammary tumor virus DNA is composed of multiple regulatory elements including binding sites for CTF/NFI and a novel transcription factor, mammary cell-activating factor. Mol. Cell. Biol. 12, 4906-4918.

Mok, E., Golovkina, T. V., and Ross, S. R. (1992). A mouse mammary tumor virus mammary gland enhancer confers tissue-specific but not lactation-dependent expression in transgenic mice. J. Virol. 66, 7529-7532.

Moriwaki, D., and Tobari, N. T. (1993). Catalog of Mutants. In DROSOPHILA ANANASSAE: Genetical and Biological Aspects, Y. N. Tobari, eds., (Tokyo, Japan: Japan Scientific Societies Press), pp 209-259.

Mozer, B. A., and Benzer, S. (1994). Ingrowth by photoreceptor axons induces transcription of a retrotransposon in the developing *Drosophila* brain. Development 120, 1049-1058.

Nusse, R. (1986). The activation of cellular oncogenes by retroviral insertion. Trends Genet. 2, 244-247.

Nusse, R. (1988). The *int* genes in mammary tumorigenesis and in normal development. Trends Genet. 4, 291-295.

Patel, R. C., and Jacobs-Lorena, M. (1992). Generation of Minute phenotypes by a transformed antisense ribosomal protein gene. J. Dev. Genet. 13, 256-263.

Pirrotta, V., Steller, H., and Bozzetti, M. P. (1985). Multiple upstream regulatory elements control the expression of the *Drosophila white* gene. EMBO J. 4, 3501-3508.

Roy, A., Lu, C. F., Marykwas, D. L., Lipke, P. N., and Kurjan, J. (1991). The *AGA1 product* is involved in cell surface attachment of the *Saccharomyces cerevisiae* cell adhesion glycoprotein a-agglutinin. Mol. Cell. Biol. 11, 4196-4206.

Rubin, G. M., and Spradling, A. C. (1982). Genetic transformation of *Drosophila* with transposable element vectors. Science 218, 348-353.

Ryerse, J. S., and Nagel, B. A. (1984). Gap junction distribution in the *Drosophila* wing mutations *vg*, *l(2)gd*, *l(3)c43^{hs1}*, and *l(2)gl^{4}*. Dev. Biol. 105, 396-403.

Sambrook, J., Fritsch, E. F., and Maniatis, T. (1989). Molecular Cloning: A Laboratory Manual, Second edition (Cold Spring Harbor, New York: Cold Spring Harbor Laboratory Press).

Sanger, F., Nicklen, S., and Coulson, A. R. (1977). DNA sequencing with chain-terminating inhibitors. Proc. Natl. Acad. Sci. USA 74, 5463-5467.

Scheidereit, C., Geisse, S., Westphal, H. M., and Beato, M. (1983). The glucocorticoid receptor binds to defined nucleotide sequences near the promoter of mouse mammary tumor virus. Nature 304, 749-752.

Selleck, S. B., Gonzalez, C., Glover, D. M., and White, K. (1992). Regulation of the G1-S transition in postembryonic neuronal precursors by axon ingrowth. Nature 355, 253-255.

Selleck, S., Nakato, H., White, K., and Easterly, N. (1994). Analysis of a novel gene required for normal cell cycle progression of lamina precursor cells. 35th Annu. Conf. Dros. Res. 59. (Abstract)

Shapiro, J. A. (1983). Mobile genetic elements (New yolk: Academic press, Inc).

Shaw, G., and Kemen, R. (1986). A conserved AU sequence from the 3' untranslated region of GM-CSF mRNA mediates selective mRNA degradation. Cell 46, 659-667.

Shrimpton, A. E., Montgomery, E. A., and Langley, C. H. (1986). *Om* mutations in *Drosophila ananassae* are linked to insertions of a transposable element. Genetics 144, 125-135.

Simpson, P. (1990). *Notch* and the choice of cell fate in *Drosophila* neuroepithelium. Trends Genet. 6, 343-345.

Tanda, S., and Corces, V. G. (1991). Retrotransposon-induced overexpression of a homeobox gene causes defects in eye morphogenesis in *Drosophila*. EMBO J. 10, 407-417.

Tanda, S., Shrimpton, A. E., Ling-Ling, C., Itayama, H., Matsubayashi, H., Saigo, K., Tobari, Y. N., and Langley, C. H. (1988). Retrovirus-like features and site specific insertions of a transposable element, *tom*, in *Drosophila ananassae*. Mol. Gen. Genet. 214, 405-411.

Tanda, S., Shrimpton, A. E., Hinton, C. W., and Langley, C. H. (1989). Analysis of the *Om(1D)* locus in *Drosophila ananassae*. Genetics 123, 495-502.

Tanda, S., Leshko, L. A., Corces, V. G., and Hori, S. H. (1993). Optic morphology (*Om*) mutations. In DROSOPHILA ANANASSAE: Genetical and Biological Aspects, Y. N. Tobari, eds., (Tokyo, Japan: Japan Scientific Societies Press), pp 89-138.

Tautz, D., and Pfeifle, C. (1989). A non-radioactive in situ hybridization method for the localization of specific RNAs in *Drosophila* embryos reveals translational control of the segmentation gene *hunchback*. Chromosoma 98, 81-85.

Tix, S., Klambt, C., and Fischbach, K. F. (1991). P-lacZ transformants as tools for the investigation of optic lobe development in Drosophila melanogaster. J. Neurogenet. 7, 149. (Abstract)

Truman, J. W., and Bate, M. (1988). Spatial and temporal patterns of neurogenesis in the central nervous system of *Drosophila melanogaster*. Dev. Biol. 125, 145-157.

von Heijne, G. (1992). Membrane protein structure prediction: hydrophobicity analysis and the positive-inside rule. J. Mol. Biol. 225, 487-494.

Wang, W., and Gralla, J. D. (1991). Differential ability of proximal and remote element pairs to cooperate in activating RNA polymerase. Mol. Cell. Biol. 11, 4561-4571.

Wharton, K. A., Yedvobnich, B., Finnerty, V. G., and Artavanis-Tsakonas, S. (1985). *opa*: a novel family of transcribed repeats shared by the *Notch* locus and other developmentally regulated loci in D. melanogaster. Cell 40, 55-62.

Wolff, T., and Ready, D. F. (1993). Pattern formation in the *Drosophila* retina. In The development of Drosophila melanogaster, M. Bate and A. M. Arias, eds., (Plainview, New Yolk: Cold spring Harbor Laboratory Press), pp 1277-1325.

Yoshida, K., Juni, N., Awasaki, T., Tsuriya, Y., Shaya, N., and Hori, S. H. (1994). Retrotransposon-induced ectopic expression of *Om(2D)* gene causes eye-specific mutation in *Drosophila ananassae*. Mol. Gen. Genet. in press.

Zhao, D.-B., Côté, S., Jähnig, F., Haller, J., and Jäckle, H. (1988). *zipper* encodes a putative integral membrane protein required for normal patterning during *Drosophila* neurogenesis. EMBO J. 7, 1115-1119.

Zipursky, S. L., Venkatesh, T. R., Teplow, D. B., and Benzer, S. (1984). Neuronal development in the Drosophila retina: monoclonal antibodies as molecular probes. Cell 36, 15-26.

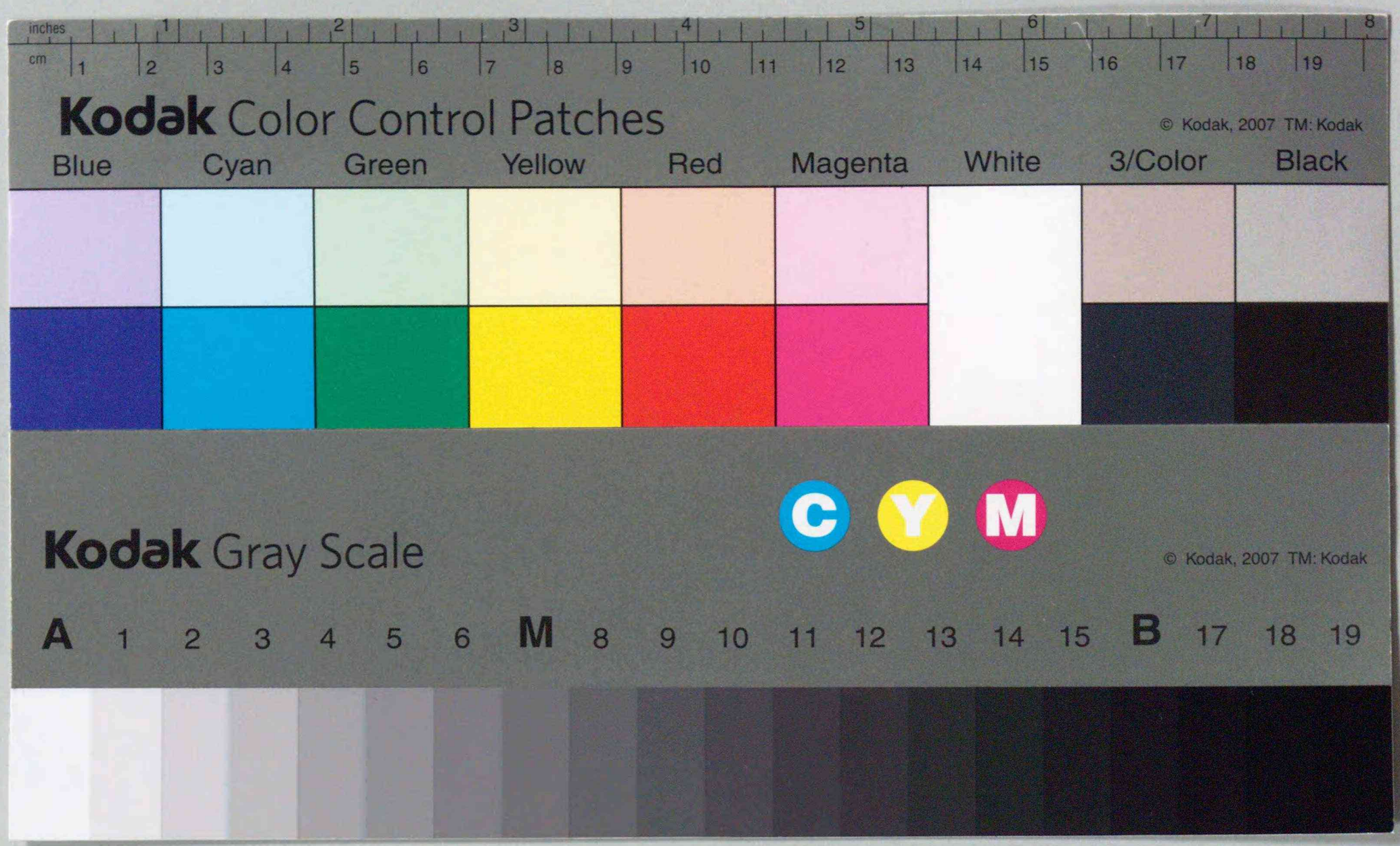
inches
cm
Kodak Color Control Patches
© Kodak, 2007 TM: Kodak
Blue
Cyan
Green
Yellow
Red
Magenta
White
3/Color
Black
Kodak Gray Scale
C
Y
M
© Kodak, 2007 TM: Kodak
A 1 2 3 4 5 6 M 8 9 10 11 12 13 14 15 B 17 18 19